Module – 2

PERFORMANCE FLIGHT TESTING - RANGE, ENDURANCE, CLIMB, TAKE OFF, LANDING, TURNING FLIGHT

Syllabus:

Performance flight testing - range, endurance and climb: Airspeed – in flight calibration. Level flight performance for propeller driven aircraft and for Jet aircraft - Techniques and data reduction. Estimation of range, endurance and climb performance.

Performance flight testing take-off, landing, turning flight: Maneuvering performance estimation. Take-off and landing - methods, procedures and data reduction.

2.1 Airspeed – Inflight Calibration

An accurate measurement of airspeed and altitude is necessary for safe flying. This is especially true for flight testing. In addition to the error caused by the airplane's instruments, several other errors are associated with the pitot-static system. This ...

2.1.1 Federal Aviation Regulaton Requirements

The FAA and its predecessors have always considered flight instrument accuracy to be important. Aeronautics Bulletin 7-A states: "The 'indicated' airspeed is defined as the speed which would be indicated by a perfect air-speed indicator, namely one which would indicate true air-speed at sea level under standard atmospheric conditions." It further refers the reader to Aeronautics Bulletin 26, section 6(A)(8), for further information on airspeed indicators. Current regulations require accuracies over specified ranges of airspeed and altitude.

2.1.2 Airspeed Errors

2.1.2.1 Position Error

When we speak of the position error of an airspeed system, we are speaking about the airspeed error caused by the failure of the static and total pressure pickups to sense the actual free stream pressures. This is caused by the location of these pickups on the airframe, hence the name position error. Considerable study has shown that the total pressure source or pitot head is relatively insensitive to inflow angles and will have little error as long as it stays within 20 deg or so of the free stream flow direction. This says that most of the position error is due to location of the static source alone. If we were to plot the static pressure variations around an airplane in flight they would look somewhat like what is shown in Fig. 3.1.

In examining this figure we can see that as the airplane approaches, the pressure increases. In the vicinity of the wing it rapidly changes from maximum positive to maximum negative. About the middle of the aft fuselage it returns to zero and then increases with the oncoming tail. Again, in the vicinity of the horizontal tail it rapidly changes sign. Then somewhere aft of the airplane it returns to free stream value. From this figure we can see that there are very few places on or around the airplane where we can get an accurate reading of the free stream static pressure. This figure also shows why static ports on many airplanes are placed on the aft fuselage. We can also see that in order to do a proper job of flight testing we must have an accurate determination of position error.

To accomplish this by flight test we use several methods. One method is the pitot-static boom located on the nose or the wing tip. To minimize position error wing tip booms should have the static source located a minimum of one chord length ahead of the wing while nose booms should have their static source at least 1.5 fuselage diameters ahead of the fuselage.

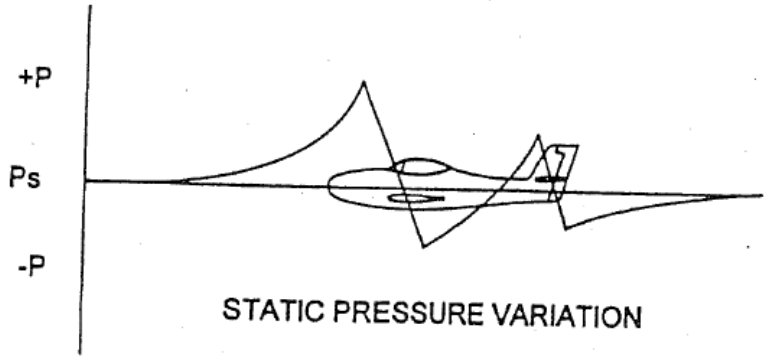

Fig. 3.1 Static pressure change with aircraft passage.

Another method is the airspeed bomb. In this method a bomblike pitot-static source is trailed far enough below and behind the aircraft to sense free stream pressures.

A third method is called the trailing cone method. In this method a trailing cone, with tubing to transmit static pressure, is trailed behind the aircraft at a distance sufficient to obtain free stream static pressure. The distance behind the aircraft of the static pressure ports should be at least 1.5 to 2 aircraft lengths behind the airplane.

All of the methods mentioned have their own set of problems. The fixed pitot-static boom becomes inaccurate at low speed when the angle to the relative wind allows total pressure to enter the static port. A free swiveling boom cures this problem but is not good at high speed due to flutter.

The trailing bomb method is only good for low-speed work since at higher speeds it tends to become unstable.

The trailing cone is good at higher speeds but has a problem with low speed since its weight will cause it to sag, introducing total pressure into the static port.

As you can see, measurement of static pressure during flight test is a sticky problem.

2.1.2.2 Lag Errors

Pitot-static systems also suffer from an error called lag error. This particular error shows up on large aircraft where the pitot-static lines are long and on

high-performance aircraft where things change rapidly. This error will also show up when either the pitot or static line is longer than the other. To correct and minimize lag errors two steps may be taken. First, attempts should be made to only obtain data during stabilized flight conditions so pressures in the pitot-static system will have time to stabilize. Second, proper attention should be paid to pitot-static system design to insure that both sides have equal volume.

2.1.2.3 Altimeter Position Error

Since the altimeter is connected to the static system, it suffers from the same position errors as the airspeed system. The altimeter is calibrated using the equation of balance of the atmosphere:

$$dp = \rho g \, dh \tag{3.10}$$

where
dp = the static pressure change
ρ = air density
g = acceleration due to gravity
dh = change in height

Then for small errors such as position error we can say:

$$\Delta P_s = -\rho g \Delta hp \tag{3.11}$$

where
ΔP_s = the static position error
Δhp = the altimeter position error in feet of pressure altitude

It is worth noting that the altimeter position is a function of altitude since the atmospheric density appears in the equation.

If the airspeed position correction is known, the altimeter position correction can be found using the equation:[7]

$$dH = 0.08865(dV_C)\left\{1 + 0.2\left(\frac{V_C}{661.5}\right)^2\right\}^{2.5}\left(\frac{V_C}{\sigma}\right) \tag{3.12}$$

where
dH = the altimeter position correction in feet
V_C = the calibrated airspeed in knots
dV_C = the airspeed position correction in knots
σ = the ambient air density ratio

2.1.3 In-Flight Calibration Methods

Several methods are currently in use for airspeed calibration. They are:

1) speed course method
2) tower fly-by method, or altimeter depression method
3) pace method
4) radar method
5) onboard reference method
6) global positioning system (GPS) method

2.1.3.1 Speed Course Method

In this method the aircraft is flown over a measured course on the ground at low altitude so an accurate measure of ground speed can be made. The course is flown in both directions and the ground speeds averaged to minimize wind errors. The average ground speed is then compared to the true flight speed and the position error is arrived at. In using this method, attempts are made to fly the course during crosswind conditions and allow the aircraft to drift. This also helps to minimize wind errors. Problems with the method are that it requires a measured course in a remote area and must be flown in very stable air so that airspeed can be maintained accurately.

2.1.3.2 Aneroid or Tower Fly-by Method

Since both the airspeed system and altimeter are hooked to the same static system on most aircraft, it is possible to relate altimeter position error directly to airspeed position error using Eq. (3.12).

In this method the aircraft flies at a constant airspeed and altitude by a tower of known height that has an observer and sensitive barometer on top. The observer can determine the aircraft height with respect to the tower using a theodolite. This height may then be compared with the height shown on the aircraft altimeter and the position error determined using Eq. (3.11). This method is almost the exclusive method used by the military and by some aerospace companies. Its problems are:

1) It has speed limitations.
2) It also requires very stable air.
3) It assumes that pitot error is zero.

2.1.3.3 Pace or Calibrated Aircraft Method

In this method another aircraft is calibrated by one of the above methods and then used as the standard for calibrating the test aircraft. This method has the advantage of safety since the calibration can be done at altitude. It also saves test time since the wait for smooth air at low altitude is not required. Its disadvantage is the requirement to maintain one aircraft in a calibrated state as the standard. The method is performed by the pace or standard aircraft maintaining a steady speed while the test aircraft flies a tight formation on the pace. When there is no relative movement in the formation the test aircraft calls "read data," and both airspeed indicators are read simultaneously. This step is repeated for several speeds through the speed range of the test aircraft.

Correction of data is straightforward. First the pace aircraft's indicated speeds are corrected to calibrated airspeed, then the test aircraft's indicated speeds are corrected for instrument error. The difference between the V_I of the test aircraft and the V_C of the pace aircraft is the ΔV_{PC} for the test aircraft.

2.1.3.4 Radar Method

The radar method is similar to the speed course method except that the times to traverse the known distance are obtained from the radar. This method has the advantage of being able to be used at altitude and it does not have the speed limitations of other methods. It does, however, require smooth air and low wind conditions. This method is flown in the same manner as the speed course method.

2.1.3.5 Onboard Reference Method

The onboard reference method consists of using an airspeed bomb or trailing cone as a reference system to calibrate the test aircraft's system. The method is performed by flying the aircraft at a number of speeds throughout its speed range and reading the indications of the test system and the reference system. Data are then reduced in the same manner as the pace method.

The advantages of this method are that it only requires one aircraft and that the reference system may be calibrated on one aircraft and then used on several other aircraft prior to requiring recalibration.

The disadvantages are that the reference system does require calibration and that a special rig or fixture is required on the test aircraft to handle the reference system.

2.1.3.6 Global Positioning Method

The global positioning system (GPS) method developed by the author replaces the ground speed obtained from the measured course in the speed course method with the ground speed along the aircraft's heading obtained from GPS ground speed and aircraft track over the Earth. By knowing the GPS ground speed, aircraft track over the ground, and the aircraft heading one can obtain the component of ground speed along the aircraft heading. Like the speed course method, the GPS method uses the ground speed measured along the heading on reciprocal headings to cancel the effects of winds and then follows the speed course procedure for data reduction to determine the pitot-static systems position correction.

The principal advantage of this method is that it can be flown at any altitude as long as the air is smooth. In addition, the aircraft only needs to be stable on altitude and airspeed long enough for the GPS receiver to update—usually a matter of seconds—before data can be read and the opposite heading established.

It should be noted that it is not necessary to have a differential GPS receiver to use this method since its accuracy is quite high with conventional receivers. This is because the ground speed taken from the GPS receiver is the first derivative of the position so a fixed error in the location of the aircraft will not affect the ground speed.

2.2 Level flight performance for propeller driven aircraft

There are a number of methods for level flight performance data reduction for propeller-driven airplanes. Most of these methods have problems with determining full throttle performance under standard conditions and are not readily useable for determining airplane drag coefficients. The method we will discuss here solves both of these problems. This method is called the PIW-VIW method.

2.2.1 Federal Aviation Administration Requirements

There are no FAA requirements for level flight performance. However, some of the acceptable methods for FAA climb performance require the use of parameters derived from the airplane drag polar which is obtained from level flight performance.

2.2.2 PIW-VIW Method

The PIW-VIW[1] method is derived by making the power required curve a single curve good for all air densities and airplane weights. To accomplish this we will make two assumptions. The first assumption is that at a given angle of attack both the lift coefficient C_L and the drag coefficient C_D are constant. When we assume that the angle of attack is the same for two different conditions of weight and altitude we can equate these two conditions through the following:

$$\frac{W_S}{W_T} = \frac{L_S}{L_T} = \frac{1/2\rho_{SL}\sigma_S V_S^2 S C_L}{1/2\rho_{SL}\sigma_T V_T^2 S C_L} \tag{9.1}$$

where
subscript S = standard conditions
subscript T = test conditions

If we cancel like terms through division and solve for the standard airspeed (V_S) which we will call VIW, and replace the true airspeed V_T and $\sqrt{\sigma}$ with equivalent airspeed V_e we have:

$$VIW = \frac{V_e}{\sqrt{W_T/W_S}} \tag{9.2}$$

The equivalent airspeed can be replaced by calibrated airspeed at low speeds and altitudes.

The power term, PIW, can be determined by assuming that the drag coefficient is constant at that angle of attack and using a similar mathematical approach to that used for VIW.

$$\frac{THP_S}{THP_T} = \frac{V_S/550(C_D 1/2\rho_{SL}\sigma_S V_S^2 S)}{V_T/550(C_D 1/2\rho_{SL}\sigma_T V_T^2 S)} \tag{9.3}$$

where
THP = the thrust horsepower and the subscripts have the same meaning as above

If we cancel like terms through division and substitute the VIW value for V_S we have:

$$THP_S = THP_T(W_S/W_T)^{3/2}\sigma_T^{1/2} \tag{9.4}$$

If we assume constant propeller efficiency, which is not a bad assumption for constant speed propellers on the front side of the power required curve, we can replace thrust horsepower with brake horsepower, BHP. Then by inverting the weight term we can rewrite the equation as:

$$PIW = \frac{\mathrm{BHP}_T\sqrt{\sigma_T}}{(W_T/W_S)^{3/2}} \tag{9.5}$$

Plotting PIW vs VIW provides one curve good for all air densities and airplane weights. It is the curve that the airplane would construct if flown at the standard weight (normally selected as the maximum takeoff gross weight) at sea level on a standard day.

2.2.3 Flight Test Method

The flight tests for level flight performance are simple and easy to perform. Testing should be conducted in smooth air as turbulence makes obtaining data difficult and will cause an apparent reduction in cruise airspeed for a given power setting. Clear, early mornings are preferred times to collect data since the air is usually smooth at all altitudes. As long as calibrations exist on the ship's instruments, they may be used for data collection and the data hand recorded. Nothing happens very fast during level flight performance tests so automatic data recording devices are not necessary.

2.2.3.1 Method for Constant Speed Propeller Driven Airplanes

For these aircraft, the test is initially conducted at maximum cruise rpm beginning at low altitude.

The procedure is to first stabilize at as low an airspeed as possible at the test altitude and record the ambient temperature. This provides an ambient temperature reading with little ram rise. Then the aircraft is accelerated at full throttle and maximum cruise rpm to maximum level flight speed. This may take some time (5 min or more). Once stabilized at maximum level flight speed, the following data is recorded:

1) airspeed
2) altitude
3) ambient temperature
4) rpm
5) manifold pressure (or torque for turbo-prop aircraft)
6) fuel quantity (for test weight determination)
7) fuel flow
8) carburetor air temperature (if available)

Once the data are collected, the manifold pressure is reduced an increment of 1 or 2 in. Hg, the airspeed allowed to stabilize, and the data collected once again. This procedure is repeated until the aircraft reaches the back side of the power required curve where the manifold pressure must be increased to maintain altitude and achieve a lower airspeed. It is worthwhile to obtain one or two data points on the back side of the power required curve. Data should be read in the sequence shown above and repeated in that sequence for each data point. The test should be repeated at medium and high altitudes to obtain a good data sample. After completing the high altitude test, full throttle manifold pressure should be obtained at each altitude during the descent so a manifold pressure vs pressure altitude curve can be obtained. If a secondary cruise rpm value is going to be given in the Pilot's Handbook, then the test should be repeated at this rpm.

2.2.3.2 Methods for Fixed-Pitch Propeller Driven Airplanes

The method for fixed-pitch propeller-driven airplanes is the same as for constant speed propeller airplanes except that rpm will change with each change in manifold pressure. Also on these airplanes, the low and medium altitude tests will be limited by maximum allowable rpm.

2.2.4 Reduction of Observed Data

The data reduction methods for propeller-driven airplanes can be divided into 1) those for constant speed propeller-driven airplanes; and 2) those for fixed-pitch propeller-driven airplanes.

2.2.4.1 Constant Speed Propeler

For airplanes with a constant speed propeller we use the PIW vs VIW method to reduce our data. In this method we must first determine our equivalent airspeed V_e (calibrated airspeed may be used for low speed airplanes), and our installed BHP at the test point. This is accomplished using the methods previously discussed in the chapters on airspeed calibration and determining engine power in-flight.

The second step in the reduction process is to determine the test density ratio σ. To accomplish this we use the equation:

$$\sigma = \delta/\theta \tag{9.6}$$

where
δ = pressure ratio (P_a/P_{SL})
θ = temperature ratio (T_a/T_{SL})

The pressure ratio can be obtained from a table lookup, entering the table with the calibrated pressure altitude Hp_C or by the equation given in Chapter 1.

The temperature ratio can be obtained by first determining the absolute temperature at the test altitude:

$$T_a = OAT_C + 273.16 \tag{9.7}$$

where
T_a = absolute temperature at the test altitude in degrees Kelvin
OAT_C = calibrated outside air temperature in degrees Celsius

and then dividing by the standard absolute temperature at sea level.

Once we have determined the test density ratio σ_T, the third step is to determine the test aircraft weight and the weight ratio W_T/W_S.

The next step is to determine values for PIW and VIW using Eq. 9.5 and 9.2 where all values are at the test data point.

We then plot the values of PIW and VIW for each data point as shown in Fig. 9.1.

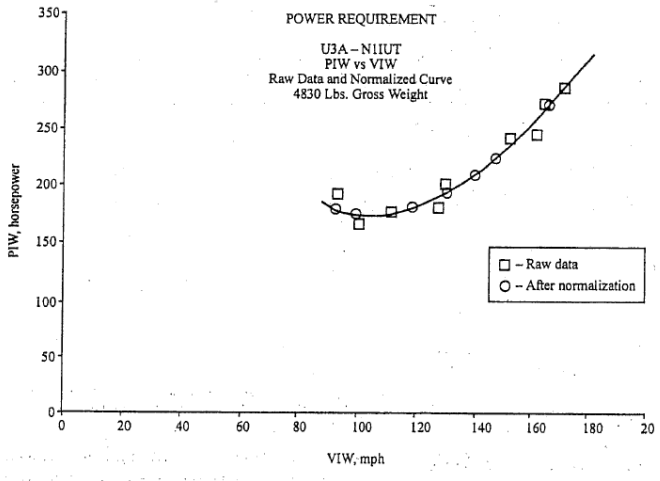

Fig. 9.1 PIW-VIW plot for a Cessna U3A. Reprinted with permission from Commander Aircraft.

2.2.4.2 PIW vs VIW Normalization

Since the values of PIW and VIW obtained above have data scatter and the proper fairing of a curve may be difficult, a normalization technique is used to make the curve into a straight line. It is then somewhat easier to fair a curve through the scattered data. We accomplish this mathematically by multiplying both PIW and VIW by VIW. This equation then becomes:

$$PIW \times VIW = f(VIW^4) \tag{9.8}$$

If we plot this equation we have a straight line as shown in Fig. 9.2. This plot does become nonlinear on both ends. On the high-speed end when our airplane is fast enough to encounter the transonic drag rise and on the low-speed end where we start to get flow separation. At all other speeds it is a straight line, and useful in data fairing. Once we have obtained this straight line plot, we then read points from it, reconvert them to values of PIW and VIW, and use these values for our faired line in Fig. 9.1. We then have a smooth curve faired through the scattered data points.

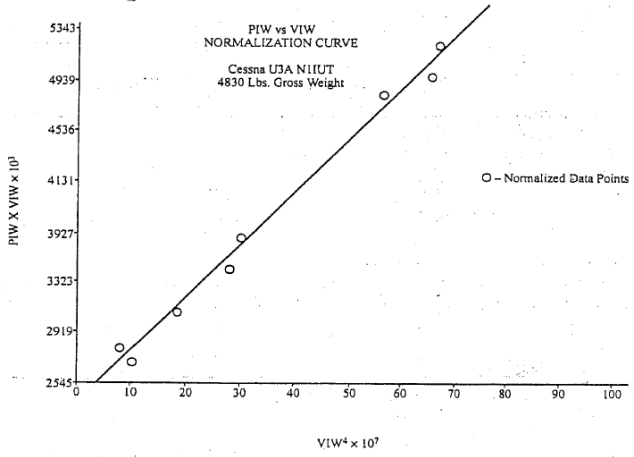

Fig. 9.2 PIW-VIW normalization from data of Fig. 9.1. Reprinted with permission from Commander Aircraft.

2.2.4.3 Fixed-Pitch Propeller

For airplanes with fixed-pitch propellers the change in rpm is so great with change in power that we can no longer assume propeller efficiency to be constant. Also, since rpm is the only power parameter with which the pilot has to work, it is necessary to have some method to relate the power the engine is developing to the rpm. We accomplish this and account for the changes in propeller efficiency by correcting the rpm for density and weight in a manner similar to that used for the PIW and VIW terms and call it NIW.

$$NIW = \frac{rpm_I \sqrt{\sigma_T}}{\sqrt{W_T / W_S}} \tag{9.9}$$

We then plot these variables into three plots as shown in Figs. 9.3, 9.4, and 9.5.

Fig. 9.3, the plot of PIW vs VIW, is only used for developing a part of the maximum power performance since for all other powers we must be able to correlate rpm and power.

Fig. 9.4, the plot of PIW vs NIW, gives us the method of relating the engine power to the rpm.

Fig. 9.5, the plot of NIW vs VIW, allows us to determine the airspeed for a handbook performance plot.

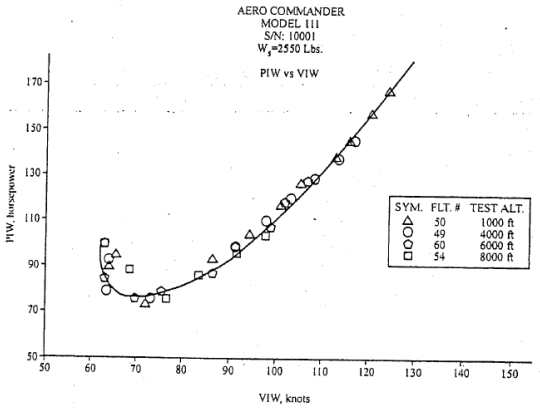

Fig. 9.3 PIW-VIW plot for determining maximum power performance. Reprinted with permission from Gulfstream Aerospace Corporation.

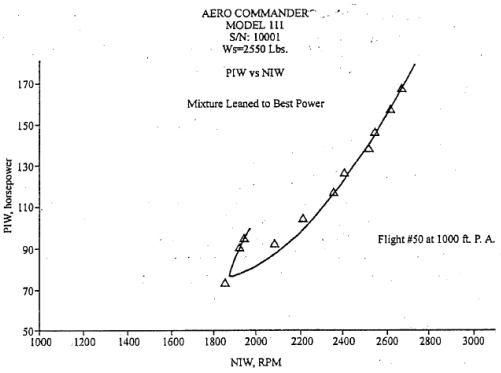

Fig. 9.4 PIW-NIW standardized power chart for a fixed pitch propeller airplane. Reprinted with permission from Gulfstream Aerospace Corporation.

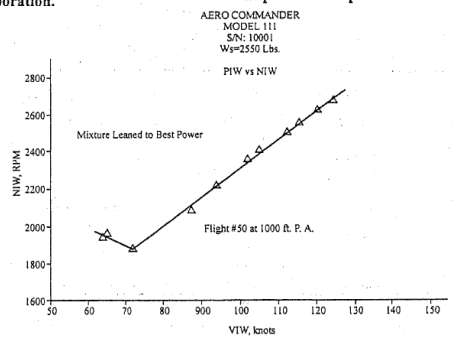

Fig. 9.5 NIW-VIW plot standardized rpm vs standardized airspeed. Reprinted with permission from Gulfstream Aerospace Corporation.

2.3 Level flight performance for Jet aircraft (Flight Test Techque for Speed Power Test of a Jet Aircraft)

The level flight performance tests of jet-powered aircraft serve the same function as those for propeller-driven aircraft. The primary purpose for conducting these tests is to provide cruise data for the "Pilot's Operating Handbook" or flight manual. However, there are several other reasons that we may wish to conduct these tests; they are:

1) to assure design specifications are met
2) to determine the airplane drag polar
3) to determine engine characteristics in flight
4) to determine drag increments of small changes during development testing

The flight test techniques and theory of level flight performance tests of jet aircraft are similar in some respects to those for propeller-driven aircraft, but there are also some important differences. First let us examine the theory behind the level flight performance of a jet aircraft.

2.3.1 Theory

If we start with the condition of steady state level flight where lift equals weight we can say:

$$L = W = \frac{\rho V_T^2 S C_L}{2} \qquad (10.1)$$

If we also consider that $V_T = Ma$, and that $a = \sqrt{\gamma P_a/\rho}$, then we can write:

$$V_T^2 = M^2 \gamma \frac{P_a}{\rho} \qquad (10.2)$$

where
M = Mach number
P_a = the ambient pressure
γ = specific heat ratio for air
a = the speed of sound
By substitution:

$$W = \frac{SC_L M^2 \gamma P_a}{2} \tag{10.3}$$

If we multiply Eq. (10.3) by P_{SL}/P_{SL} and substitute the pressure ratio δ for P_a/P_{SL}, then Eq. (10.3) becomes:

$$W = \frac{SC_L M^2 \gamma \delta P_{SL}}{2} \tag{10.4}$$

and by rearranging we have:

$$C_L = \frac{2(W/\delta)}{\gamma P_{SL} M^2 S} \tag{10.5}$$

For a given aircraft and set of conditions, γ, P_{SL}, and S are constants. Therefore:

$$C_L = f\left(\frac{W}{\delta}, M\right) \tag{10.6}$$

By the same approach an equation similar to Eq. (10.5) can be obtained for the drag coefficient:

$$C_D = \frac{2(D/\delta)}{\gamma P_{SL} M^2 S} \tag{10.7}$$

and likewise:

$$C_D = f\left(\frac{D}{\delta}, M\right) \tag{10.8}$$

Then if we have the engine thrust characteristics, the level flight data can be converted to values of C_D and C_L for the construction of an airplane drag polar. Once we have the airplane drag polar, we can calculate airplane performance characteristics for flight manual or other uses.

However, in many instances it is simpler if we have relationships that do not require the determination of C_L and C_D. If we rewrite Eq. (10.8) as:

$$D/\delta = f(C_D, M) \tag{10.9}$$

and say that:

$$C_D = C_{DP} + C_{Di} \tag{10.10}$$

we know that $C_{Di} = f(C_L)$, so also must:

$$C_D = f(C_L) \tag{10.11}$$

If we replace C_L in Eq. (10.11) with its function from Eq. (10.6), we have:

$$C_D = f\left(\frac{W}{\delta}, M\right) \tag{10.12}$$

or:

$$D/\delta = f(C_D, M) = f\left(\frac{W}{\delta}, M\right) \tag{10.13}$$

We now have created a functional relationship for drag which combines the aircraft and engine performance characteristics.

The variables that affect engine thrust are:

1) velocity (V)
2) temperature (T)
3) pressure (P)
4) engine speed (N)
5) engine size (D)

If we evaluate the variables using the Buckingham Π Theorem of dimensional analysis we can say:

$$\frac{F}{PD^2} = f\left(\frac{V}{\sqrt{T}}, \frac{ND}{\sqrt{T}}\right) \tag{10.14}$$

Since the engine size D is fixed we may eliminate it. We may also replace $V/\sqrt{T}$ with Mach number M and reference all pressures and temperatures to sea level by use of the temperature ratio θ and the pressure ratio δ. Eq. (10.14) then becomes:

$$\frac{F_N}{\delta} = f(M, N/\sqrt{\theta}) \tag{10.15}$$

A similar analysis will also show:

$$\frac{Q\sqrt{\theta}}{\delta} = f(M, N/\sqrt{\theta}) \tag{10.16}$$

where
Q = the mass flow of air through the engine

$$\frac{W_f}{\delta\sqrt{\theta}} = f(M, N/\sqrt{\theta}) \tag{10.17}$$

where
W_f = fuel flow

On engines which have the capability of reading engine pressure ratio (EPR), the value $N/\sqrt{\theta}$ may be replaced by EPR in Eqs. (10.15) through (10.17).

Since in level flight thrust is equal to drag, we can say:

$$f(M, N/\sqrt{\theta}) = f\left(\frac{W}{\delta}, M\right) \tag{10.18}$$

From this relation comes:

$$M = f\left(\frac{W}{\delta}, \frac{N}{\sqrt{\theta}}\right) \tag{10.19}$$

This relationship is quite important since it is the basis for the speed power level flight method for jet aircraft. If the pilot holds W/δ constant by varying his test altitude as weight changes, he may then obtain a plot of how Mach number varies with power setting (Fig. 10.1). Since all of the parameters are interrelated, a whole series of plots may be obtained using these basic relationships. Examples are shown in Figs. 10.2–10.6.

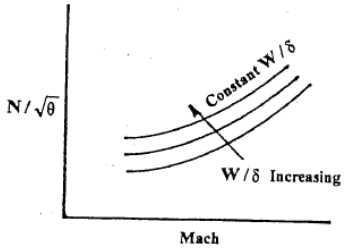

Fig. 10.1 Referred rpm vs Mach.

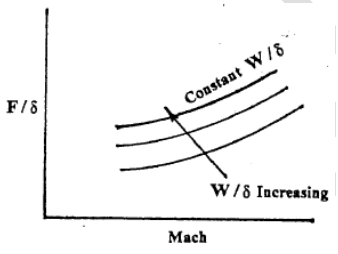

Fig. 10.2 Referred thrust vs Mach.

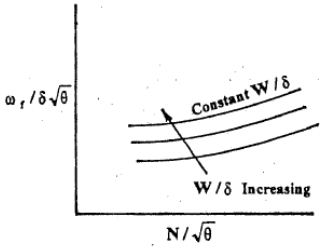

Fig. 10.3 Referred fuel flow vs referred rpm.

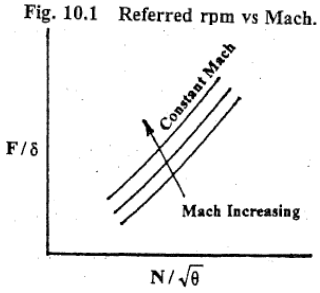

Fig. 10.4 Referred thrust vs referred rpm.

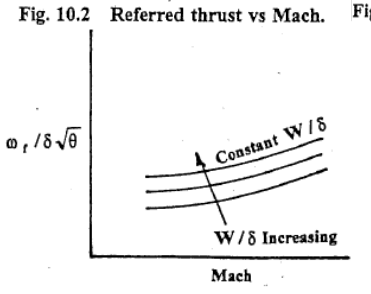

Fig. 10.5 Referred fuel flow vs Mach number.

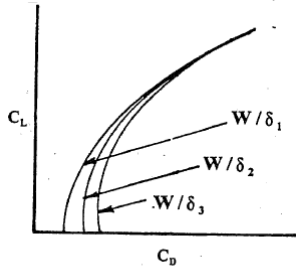

Fig. 10.6 Drag polar.

2.3.2 Flight Test Technique

As might be expected from the past discussion, the flight test technique for the speed power test of a jet aircraft is somewhat different from that for a propeller-driven aircraft. Since we intended to plot our data at values of constant W/δ, we must vary our test altitude as we burn off fuel in order to keep W/δ constant. This requires considerably more preflight planning than is required for level flight tests of propeller-driven airplanes. It also requires considerable skill on the part of the test pilot since a missed point cannot be repeated without an altitude change. The test is best performed by a pilot and flight test engineer working as a team. Even in single seat aircraft this can be accomplished via radio link.

In order to perform the test, the crew will need a plot of altitude vs aircraft weight for a constant W/δ (Fig. 10.7). They will also need a plot of the altimeter position error vs Mach number. The test team must determine the altitude at which the test data point is to be flown and allow sufficient time for the aircraft to arrive at that altitude and stabilize. This time averages about 8 min per data point.

In planning the test, estimate the airplane weight at the first data point, and then enter the altitude vs weight chart and find the aim altitude. This altitude must then be corrected for instrument and position error to give the pilot an aim indicated altitude. High-speed points should be obtained first, and then the speed reduced for each successive point. This seems to be the most efficient technique since some of the excess speed can be used in the climb. Also, most aircraft seem to stabilize faster when the data point is approached from the high-speed side.

Once established at the aim altitude, with the airspeed stabilized, allow 2–3 min to elapse after the last throttle movement before taking data. This will permit the engine to thermally stabilize. The rate of climb and aircraft acceleration should be zero. However, an acceptable tolerance is rate of climb less than 100 ft/min and airspeed 1.5 kn in 2 min. Even light turbulence will cause excursions greater than this and should be avoided.

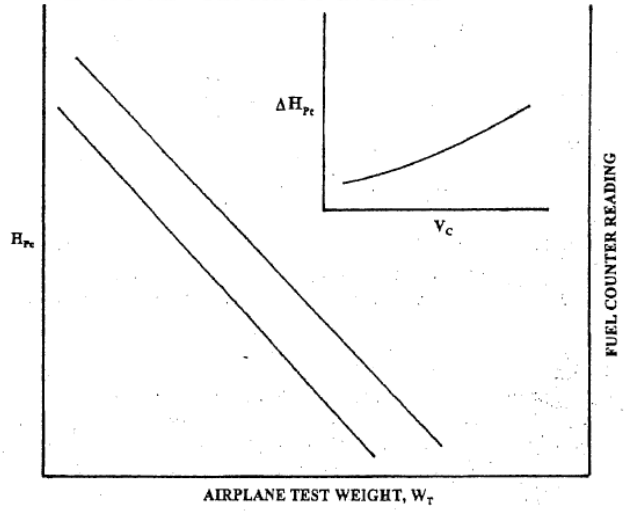

Fig. 10.7 Plot calibrated pressure altitude vs test weight for a constant W/δ.

2.3.3 Data Reduction

The data reduction sequence used for reducing the data obtained during the speed power tests will depend to a degree upon the type of jet engine in the aircraft and the way it is instrumented. For instance, the data from a straight turbojet-powered aircraft is handled differently than data from a turbofan engine. Also, if pressure ratio instrumentation is available the data is reduced in a different manner than if this instrumentation is not available.

All of these sequences are covered in the reference material, and due to the number and length we will not discuss them here.

2.4 Range and Endurance

The airplane's ability to cover great distances by conversion of fuel energy into airspeed and its ability to use this same energy to stay aloft over a period of time are performance parameters of great importance. They take on even greater importance when one considers the dwindling world supplies of petroleum energy and the cost of acceptable substitutes.

The first of the above mentioned performance parameters we call range. The range parameter can be described in two different ways. First, the problem of flying a given distance with a minimum expenditure of fuel. Another method to describe this problem is the ability to obtain the maximum flying distance from a given fuel load. Either of these problems is approached the same way by the pilot, and it is the task of the test pilot and flight test engineer to provide the pilot with the information necessary to master them.

Second, the performance parameter of staying aloft for the maximum time on a minimum amount of fuel is called endurance. This parameter becomes important when the airplane must hold due to traffic delays and in certain other aircraft applications such as fish spotting or antisubmarine warfare missions that require long periods of time on station.

A convenient method for expressing the range, or endurance of an airplane is by the use of specific range and specific endurance.

Specific range can be defined in several ways as is shown below:

$$SR = \frac{\text{nautical miles traveled}}{\text{pounds of fuel consumed}} \tag{11.1}$$

or

$$SR = \frac{V_T}{\omega_F} \tag{11.2}$$

where
SR = specific range
V_T = true airspeed in knots
ω_F = fuel flow in pounds per hour

From Eq. (11.2) we can see that if we obtain values of fuel flow at the same time we are collecting other performance data, then we have the information for determining specific range.

Since range involves flying a distance while endurance involves flying a time, the specific endurance, SE, can be defined as:

$$SE = \frac{\text{hours flown}}{\text{pounds of fuel consumed}} \tag{11.3}$$

or

$$SE = \frac{1}{\omega_F} \tag{11.4}$$

If we recall our level flight performance theory, we will remember that the performance for propeller-driven airplanes is determined from a plot of THP vs V_e called the power required curve. Performance for the jet airplane, however, is determined from the thrust vs V_e curve. Since power is a function of both thrust and velocity, it is easy to see the relationships developed from the power required curve are going to be somewhat different than those developed from the thrust required curve. It is for this reason that we shall discuss range and endurance for propeller-driven airplanes and for jet airplanes separately.

2.4.1 Range – Propeller Driven Airplanes

The propeller-driven airplane obtains its thrust by combining the propeller with one of three types of powerplants:

1) normally aspirated reciprocating
2) turbocharged or supercharged reciprocating
3) gas turbine

The fuel flow for each of these types is more directly a function of the horsepower delivered to the propeller than to the thrust produced. Also, the

fuel flow characteristics of each of these types is somewhat different so we will address each type separately. First, let us review the range theory for propeller-driven airplanes.

2.4.1.1 Propeller Driven Airplane Range Theory (Breguet Range Equations)

The equations for range were first published by L. Breguet and are known as the Breguet range equations. They are based on the fact that an increment of range ds is equal to the velocity of the vehicle V_T times the increment of time traveled dt

$$ds = V_T\,dt \tag{11.5}$$

and that for a propeller-driven aircraft the weight of fuel consumed in a given time is a function of the specific fuel consumption c and the power developed P.

$$dW = cP\,dt \tag{11.6}$$

If we solve Eq. (11.6) for dt and substitute it into Eq. (11.5) we have:

$$ds = \frac{-V_T\,dW}{cP} \tag{11.7}$$

or

$$R = \int ds = \int_{W_2}^{W_1} \frac{V_T\,dW}{cP} \tag{11.8}$$

where
R = range
W_1 = initial gross weight
W_2 = final gross weight

Since power for a propeller-driven airplane can be expressed as:

$$P = \frac{DV_T}{\eta_P} \tag{11.9}$$

where
D = airplane drag
η_P = propeller efficiency

and in level flight $L = W$. We can state Eq. (11.8) as:

$$R = \int_{W_2}^{W_1} \left(\frac{\eta_P}{c}\right)\left(\frac{L}{D}\right)\frac{dW}{W} \tag{11.10}$$

If we integrate Eq. (11.10) and express range in nautical miles and c in pounds per BHP-hours then we have the Breguet range equation:

$$R = 325.8\left(\frac{\eta_P}{c}\right)\left(\frac{C_L}{C_D}\right)\log_e\frac{W_1}{W_2} \tag{11.11}$$

If we want to express this equation in terms of specific range, we have:

$$SR = \frac{dR}{dW} = 325.8\left(\frac{\eta_P}{c}\right)\left(\frac{C_L}{C_D}\right)\left(\frac{1}{W}\right) \tag{11.12}$$

In evaluating Eq. (11.11) we can see that the specific range will be at a maximum when we have a maximum value for the combined term of $(\eta_P/c)(C_L/C_D)$. Keeping this in mind let us see how this is affected by each type of powerplant.

Normally Aispirated Reciprocating Powerplants

In evaluating reciprocating engine powered airplane range performance, it is useful to return to evaluating the effect of various parameters on the power required curve. Fig. 11.1 is a typical power required curve. The maximum range occurs at the point where a straight line from the origin is tangent to the curve. This is the point on the curve where the velocity achieved per unit power is the greatest. It is also the point where the maximum L/D occurs.

As altitude increases the power required curve (when plotted vs V_T) moves up and to the right as is shown in Fig. 11.2. So, as altitude increases, we get an increase in the true airspeed V_T and the power required P_{REQ} to maintain that true airspeed. If the true airspeed and power required for best range are known at one altitude they may be obtained for other altitudes by use of the following relations:

$$V_{T_{ALT}} = V_{T_{SL}}\sqrt{\frac{\sigma_{SL}}{\sigma_{ALT}}} \tag{11.13}$$

$$P_{REQ_{ALT}} = P_{REQ_{SL}}\sqrt{\frac{\sigma_{SL}}{\sigma_{ALT}}} \tag{11.14}$$

For a normally aspirated reciprocating engine at cruise power settings, the fuel flow is a function of engine power. This information and Eqs. (11.13) and (11.14) would indicate that the specific range for a normally aspirated reciprocating engine powered propeller-driven airplane would be unaffected by altitude. Except for the cases where fuel flow or propeller efficiency vary significantly with altitude, this is a true statement.

Now let us return to the power required curve and evaluate the effects of fuel burn-off, or weight change, on the specific range. Fig. 11.3 shows the effects of weight change on the power required curve, and the point of $(L/D)_{max}$. As we can see from this figure, the power required curve moves down and to the left as weight decreases. This says that the largest value of specific range occurs at the minimum flight weight and that the airspeed and power combination to achieve maximum specific range continually changes throughout the flight. The effects of weight on range related variables for the propeller-driven airplane may be determined by use of the following relations:

$$V_{e(W_2)} = V_{e(W_1)}\sqrt{\frac{W_2}{W_1}} \tag{11.15}$$

$$P_{REQ(W_2)} = P_{REQ(W_1)}\left(\frac{W_2}{W_1}\right)^{3/2} \tag{11.16}$$

$$SR_{(W_2)} = SR_{(W_1)}\left(\frac{W_2}{W_1}\right) \tag{11.17}$$

where
W_1 = aircraft gross weight at the initial condition
W_2 = aircraft gross weight at the condition in question

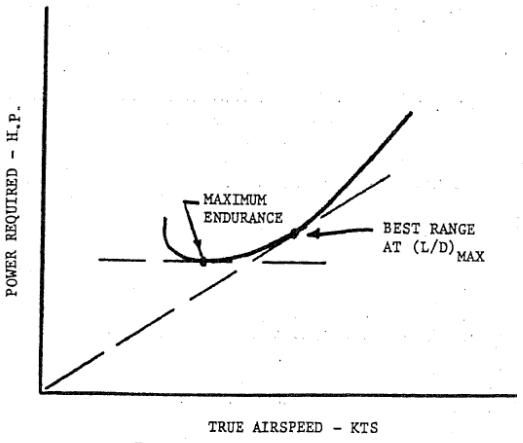

Fig. 11.1 Typical power required curve.

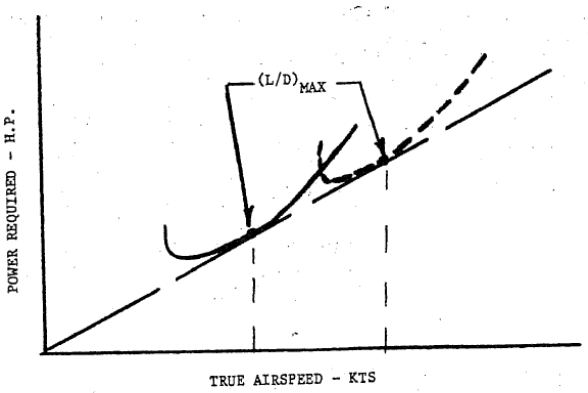

Fig. 11.2 Effects of altitude on power required and airspeed for best range.

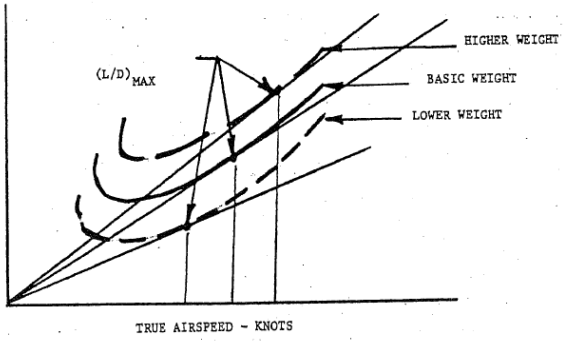

Fig. 11.3 Effects of weight on power required and airspeed for best range.

What we have just been discussing were the airframe effects, or the effects of various parameters on the L/D term of the Breguet range equation. Now lets turn our attention to the (η_P/c) term. The brake specific fuel consumption c for a normally aspirated reciprocating engine at cruise power settings is normally a constant. In other words the fuel flow will increase linearly with increased power. It does not vary significantly with altitude. This would say that the (η_P/c) term on a normally aspirated engine-powered, propeller-driven airplane is only affected by changes in propeller efficiency.

Propeller efficiency η_P is affected by a number of variables. Power, rpm, altitude, and aircraft velocity all have an effect on the propeller efficiency. The effects of these variables are all interrelated and it is difficult to determine which one will have the most powerful effect. This is especially true on a constant-speed propeller since the sensing mechanism adjusts the blade angle to maintain the rpm and not necessarily to operate at the most efficient angle. It is for this reason, that for range determination, it is preferred to obtain speed-power information at several values of rpm and altitude in order to determine the best combination.

Turbocharged Reciprocating Engine

Any range advantage from the turbocharged engine will come from its ability to operate a high altitude at cruise power settings and high true airspeeds. This advantage may be eliminated by the climb fuel requirement, and if the engine requires a higher brake specific fuel consumption in order to cool. Other aspects of the range of turbocharged engine powered airplanes are similar to the normally aspirated engine powered airplanes.

One additional advantage of the turbocharged engine powered airplane is that it may climb to altitudes where the prevailing winds are stronger and achieve some additional range advantage. The effects of wind on range will be discussed in detail later.

Turboprop Engines

The range of an airplane using a turboprop engine is affected by both the aircraft aerodynamics and the operating characteristics of the turbine engine.

From the aerodynamic standpoint the variables affecting range are the same as other propeller-driven airplanes.

The engine operating characteristics are quite different, however. For best fuel efficiency the turbine engine demands air at low temperature. This makes the turbine engine operate most efficiently at high altitude where the air temperature is low. In addition, the turbine engine is more efficient at higher power settings, and since the power required to achieve best range increases with altitude this, too, makes the turboprop engine more efficient at high altitude.

Since the propeller-driven airframe prefers low altitude for best range, while the turboprop engine prefers high altitude, the combination turboprop airplane will achieve its best range at some intermediate altitude. This makes flight testing for range determination more of a chore on turboprop airplanes than on other propeller-driven airplanes.

2.4.2 Range – Jet Aircraft

The range of a turbojet or fan-jet powered aircraft is affected by a larger number of variables than is the range of a propeller-driven aircraft. For instance, the specific fuel consumption of the jet engine is dependent upon the thrust being developed, the air density and temperature, and the speed of the aircraft. The operational envelope of a jet aircraft also affects its range. This is especially true of an aircraft that is capable of operating at supersonic speeds. For instance, aircraft designed for cruise at supersonic speeds may achieve best range while operating supersonic. The reverse would be true for those aircraft with supersonic capability that are designed for operation primarily at subsonic speeds.

Since so many variables do exist, let us divide them into those related to airframe and to powerplant as we did with propeller-driven airplanes.

First let us examine the aerodynamic theory relating to the range of a jet aircraft.

The fuel flow of a jet engine is primarily dependent upon the thrust produced rather than upon power as was the case for the propeller-driven airplane. This leads us to evaluate the range of the jet aircraft by use of the thrust required curve rather than by power required. Fig. 11.4 is a typical plot of thrust required for a subsonic jet aircraft. The best range point is located where a straight line from the origin is tangent to the curve. This point on the curve occurs where the ratio of the square root of the lift coefficient over the drag coefficient is at a maximum $(\sqrt{C_L}/C_D)_{max}$. At this point the induced drag is roughly 25% of the total drag. The jet airplane, therefore, is not nearly so dependent upon high aspect ratio wings for good range performance as is the propeller-driven airplane where best range occurs at $(L/D)_{max}$.

Let us now derive the range equations for a jet aircraft to determine why the difference between props and jets exist. The weight change of a jet aircraft due to fuel consumption can be expressed by the equation:

$$dW = c_t T\, dt \qquad (11.18)$$

where
dW = weight change due to fuel consumption
c_t = thrust specific fuel consumption in pounds of fuel/(lb thrust/s)
T = thrust in pounds
dt = time of flight in seconds

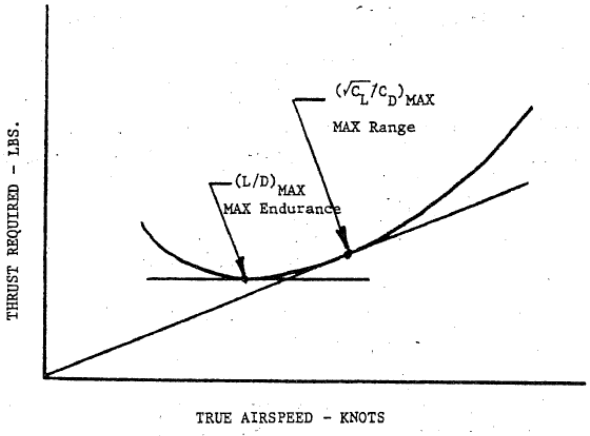

Fig. 11.4 Typical thrust required curve.

By solving for dt and substituting the result into the incremental range equation [Eq. (11.5)] we have:

$$ds = \frac{V_T\, dW}{c_\tau T} \tag{11.19}$$

and

$$R = \int_{W_2}^{W_1} \frac{V_T\, dW}{c_\tau T} \tag{11.20}$$

In level flight thrust is equal to drag and drag may be shown equal to:

$$T = D = W\left(\frac{C_D}{C_L}\right) \tag{11.21}$$

and true airspeed V_T is equal to:

$$V_T = \sqrt{\frac{2W}{\rho C_L S}} \tag{11.22}$$

By substitution of these identities into Eq. (11.20) and integrating we have:

$$R = \frac{2.828}{c_\tau\sqrt{\rho S}}\left(\frac{\sqrt{C_L}}{C_D}\right)\left(\sqrt{W_1} - \sqrt{W_2}\right) \tag{11.23}$$

Eq. (11.23) gives the range in ft. If we convert this to nautical miles and the thrust specific fuel consumption to pounds of fuel/(lb thrust h) we have:

$$R = \frac{1.674}{c_\tau\sqrt{\rho S}}\left(\frac{\sqrt{C_L}}{C_D}\right)\left(\sqrt{W_1} - \sqrt{W_2}\right) \tag{11.24}$$

Eqs. (11.23) and (11.24) show that the range for a jet aircraft is a function of $\sqrt{C_L}/C_D$ rather than C_L/C_D as was the case for propeller-driven airplanes.

It also shows that jet range is very much a function of altitude since the air density ρ appears in the lower half of the equation.

If we neglect engine performance parameters the specific range SR of a jet airplane is affected by altitude according to the following relation:

$$SR_{ALT} = SR_{SL}\sqrt{\frac{\sigma_{SL}}{\sigma_{ALT}}} \qquad (11.25)$$

These effects are graphically displayed when the thrust required is plotted against true airspeed V_T and shown for several altitudes. Figure 11.5 shows that true airspeed increases with altitude while thrust required remains constant. Therefore, for a jet airplane the aerodynamic parameters contribute to an improvement in range with an increase in altitude.

Now let us turn our attention to the engine effect on the range. Engine performance of the jet engine is improved by altitude in two ways. First, an increase in altitude causes a decrease in inlet air temperature. A decrease in inlet air temperature causes a reduction in the thrust specific fuel consumption. This is true up to the tropopause where air temperature becomes constant. The second benefit of increased altitude on the performance of a jet engine is caused by the increase in engine rpm required to generate the thrust required. Jet engines operate more efficiently at higher rpm and increased altitude provides this desired effect.

From the preceding discussion we can see that the range of a jet aircraft is very dependent upon altitude. In fact, the optimum altitude for the beginning of cruise flight is the altitude where maximum continuous thrust will maintain the best range airspeed. If that altitude is maintained, the best range airspeed will decrease. This is due to the aircraft weight change with fuel burn-off.

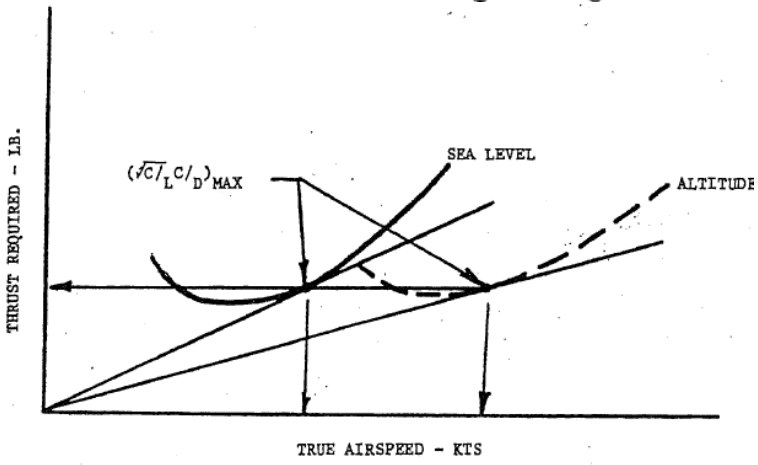

Fig. 11.5 Effects of altitude on thrust required and airspeed for best range.

Although it may be necessary to maintain a constant altitude cruise for air traffic control reasons, this is not the most efficient method for cruise flight in a jet aircraft.

If we return to the dimensional analysis method of evaluating jet aircraft performance that we used earlier for other level flight performance parameters we find that specific range may be defined as:

$$SR = \frac{\omega_f}{\delta\sqrt{\theta}M} = f(C_L, M) \qquad (11.26)$$

This equation may also be stated as:

$$SR = \frac{\omega_f}{\delta\sqrt{\theta}M} = f\left(\frac{W}{\delta}, M\right) \tag{11.27}$$

It is this last equation that gives us the key to the most efficient method of cruise operation. Since the specific range is a function of W/δ and Mach, we could hold the initial optimum condition of specific range if we held these values constant. This is accomplished by holding Mach number constant and allowing the aircraft to climb as fuel is burned so W/δ remains constant. This is the concept of the cruise climb and is the most efficient method of cruise for a jet aircraft.

If we compare the specific ranges of the constant altitude method of cruise with the cruise climb we find the specific ranges vary according to the following relations:

$$SR_2 = SR_1\sqrt{\frac{W_1}{W_2}} \tag{11.28}$$

for a constant altitude cruise, and

$$SR_2 = SR_1\left(\frac{W_1}{W_2}\right) \tag{11.29}$$

for a cruise climb.

These relations show the cruise climb to be a much more efficient method of operating a jet aircraft. They also help to point out the considerable difference in range performance between jet and propeller-driven airplanes.

2.4.3 Effects of Wind on Range (for both Propeller and Jet Driven Aircrafts)

The range theory we have been discussing was for the case of zero wind. Very seldom in real-life flight situations do we experience a zero wind condition. This leads us then to consider the effects of wind on aircraft range. It is easy to understand that a tailwind will increase the aircraft's range while a headwind will reduce it. The effects of headwinds or tailwinds on range may be determined by the following equation:

$$R_{WIND} = R_{NOWIND} \pm (V_{WIND})t \tag{11.30}$$

where
t = time of flight

It can be seen from Eq. (11.30) that the time of flight plays an important role in the effect of wind on airplane range. For a headwind condition we would want to reduce the flight time, and for a tailwind we would want to increase it. The method available to the pilot to accomplish this task is to increase or decrease airspeed.

The amount that the airspeed should be increased or decreased to maintain optimum range conditions may be determined by reference to Figs. 11.6 and 11.7. These figures show typical power required and thrust required curves for propeller-driven and jet aircraft. From our previous discussion we know that best range, no wind, is achieved at the airspeed where a straight line drawn

from the origin is tangent to the curve. If we plot the wind speed along the abscissa as is shown in Figs. 11.6 and 11.7, and draw a straight line from that point tangent to the curve, then the best range airspeed for that wind condition is the airspeed where the line is tangent to the curve.

For the propeller-driven airplane determining at what altitude to fly to achieve optimum range depends on the altitude where most favorable winds exist. However, there is a trade-off in the benefit derived from the wind vs the fuel required to climb to that altitude.

The jet aircraft presents a much more complicated problem when we try to determine optimum range altitude when under the influence of wind. Since the range of a jet aircraft increases with increasing altitude, it may be worthwhile to select altitudes with unfavorable winds. This of course will depend upon the trade-off between range gained with increasing altitude and range lost due to unfavorable winds.

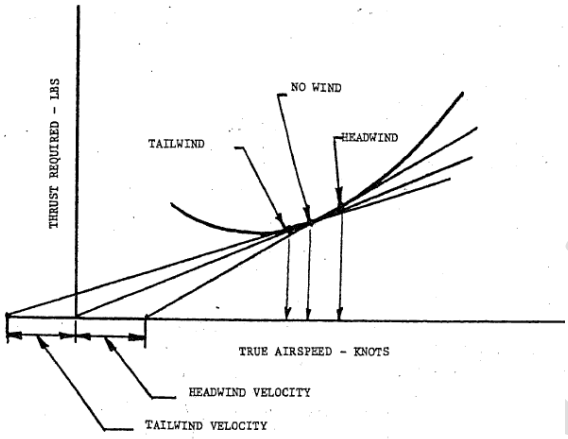

Fig. 11.6 Effects of wind on best range airspeed for a jet-propelled airplane.

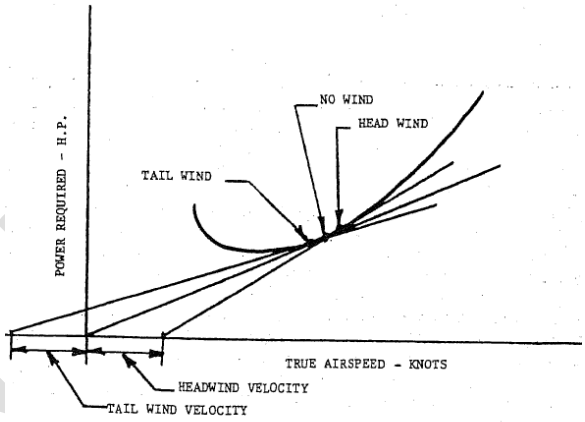

Fig. 11.7 Wind effects on best range airspeed for a propeller-driven airplane.

2.4.4 Endurance – Propeller Driven Aircraft

Now let us turn our attention from range to that of endurance or staying aloft for the maximum amount of time. As was discussed earlier the maximum endurance for an airplane occurs at the condition of level flight where fuel flow is lowest. For the propeller-driven airplane this point occurs at the minimum power required. This is shown in Fig. 11.1 for a typical propeller-driven airplane.

Breguet also determined the equations for endurance of a propeller-driven airplane. By use of Eq. (11.6) we may solve for time and derive the Breguet range equation for a propeller-driven airplane. The derivation is similar to that used for the range equation with the following results:

$$E = 778\left(\frac{\eta_P}{c}\right)\left(\frac{C_L^{3/2}}{C_D}\right)\sqrt{\rho S}\left(\frac{1}{\sqrt{W_2}} - \frac{1}{\sqrt{W_1}}\right) \tag{11.31}$$

and

$$SE = 550\left(\frac{\eta_P}{c}\right)\left(\frac{C_L^{3/2}}{C_D}\right)\left(\rho\frac{S}{2}\right)\left(\frac{1}{W^{3/2}}\right) \tag{11.32}$$

where
E and SE are in hours

From Eqs. (11.31) and (11.32) we can see that the endurance and specific endurance equations both contain a density term, and as the density decreases

the endurance also decreases. These equations hold for the reciprocating engine-powered propeller-driven airplane that achieves its best endurance at sea level.

In the case of the turboprop airplane the density term in Eqs. (11.31) and (11.32) may be canceled by engine effects. The turbine engine prefers both low inlet air temperature and high power settings for best efficiency. The trade-off between these factors and the aerodynamic factor expressed in Eqs. (11.31) and (11.32) may cause the turboprop airplane to prefer some medium altitude for best endurance.

The engines preference for high power is the reason that multiengine turboprop patrol aircraft often operate with one or more engines shutdown.

2.4.5 Endurance – Jet Aircraft

The fuel flow of a jet aircraft is a function of thrust, therefore the lowest fuel flow, and maximum endurance, will occur at the level flight point for minimum thrust. From our previous discussions of jet aircraft we know that this point occurs at $(L/D)_{max}$ (see Fig. 11.4). We also know from these discussions that the thrust required does not vary with altitude and that from the aerodynamic standpoint endurance is not a function of altitude. This may be determined mathematically by deriving the endurance equations for a jet aircraft. If we solve Eq. (11.18) for time we have:

$$dt = -\frac{dW}{c_\tau T} \tag{11.18}$$

To obtain endurance E we integrate:

$$E = \int_{W_2}^{W_1} \frac{dW}{c_\tau T} \tag{11.33}$$

If we then substitute Eq. (11.21) for thrust we have:

$$E = \int_{W_2}^{W_1} \frac{dW}{W}\left(\frac{1}{c_\tau}\right)\left(\frac{C_L}{C_D}\right) \tag{11.34}$$

which, when integrated, becomes:

$$E = \frac{1}{c_\tau}\left(\frac{C_L}{C_D}\right)\log_e \frac{W_1}{W_2} \tag{11.35}$$

and for specific endurance SE

$$SE = \frac{1}{c_\tau}\left(\frac{C_L}{C_D}\right)\frac{1}{W} \tag{11.36}$$

We can see from Eqs. (11.35) and (11.36) that the jet aircraft is insensitive to altitude aerodynamically.

As we discussed in the range section, the same is not true for the jet engine. It is the most efficient at or near the tropopause.

Considering both of these factors, the jet airplane will also achieve its greatest specific endurance at or near the tropopause.

2.5 Climb Performance Methods and Data Reduction

2.5.1 Federal Aviation Administration Regulations

The regulations for climb in CAR 3 and FAR Part 23 are divided into those for airplanes under 6000 lbs. takeoff gross weight and those in excess of 6000 lb takeoff gross weight.

For single engine airplanes, there are requirements for climb in a clean configuration, in a takeoff configuration, and in a rejected landing configuration.

For multi-engine airplanes, the requirements are for climb in a clean configuration, in an engine out configuration, and in a rejected landing configuration.

2.5.2 Test Methods

2.5.2.1 Steady Climbs

The steady climb method, also called sawtooth climbs, requires considerable flight test time to complete. First, a series of climbs are performed at various airspeeds and several altitudes. These climbs are from 3 to 5 min duration at each airspeed, and two climbs are conducted at each airspeed and altitude in opposite directions in order to cancel wind gradient acceleration effects on the rate of climb. Also, the climbs are conducted crosswind in order to help minimize wind effects. Plots of pressure altitude vs time are then made for each airspeed and altitude as shown in Fig. 13.1. An average curve is drawn between the data from opposite direction climbs, and the slope is taken at the test altitude in question to determine the rate of climb dH/dt, at the altitude, for that airspeed. This process is repeated for each airspeed and altitude and the resultant rates of climb vs airspeed are plotted as shown in Fig. 13.2. Since this data is only used to determine best rate-of-climb speed V_y and best angle-of-climb speed V_x, and these values are not significantly affected by nonstandard conditions other than weight, it is customary to ignore corrections to this data and plot the values directly. By drawing tangents to the top of each curve a plot of best rate-of-climb speed V_y vs altitude H_p may be determined as

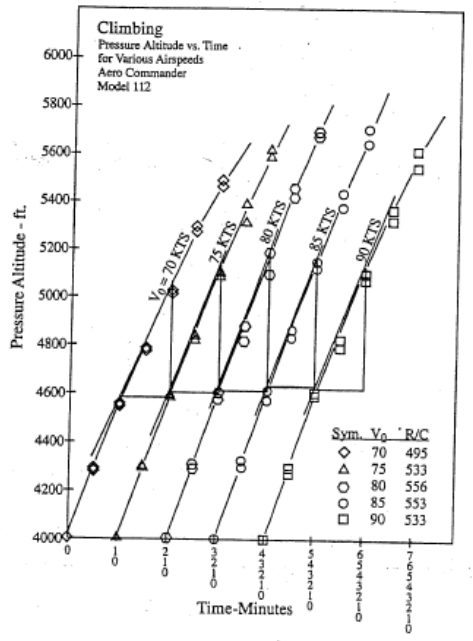

Fig. 13.1 Pressure altitude vs time for various climb airspeeds. Reprinted with permission from Commander Aircraft.

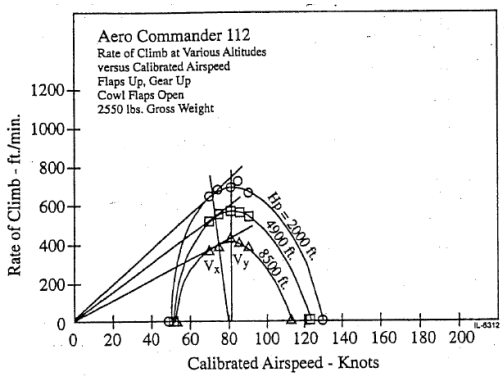

Fig. 13.2 Rate of climb vs calibrated airspeed for three altitudes. Reprinted with permission from Commander Aircraft.

shown in Fig. 13.3. By drawing lines from the origin tangent to the curves as shown in Fig. 13.2, we may also obtain a plot of best angle-of-climb speed V_x vs altitude H_p also shown in Fig. 13.3.

Once we have the best rate-of-climb speed V_y, we then conduct climbs at several altitudes using only this speed. These climbs are sometimes referred to as check climbs. Again, we conduct the climbs in opposite directions (cross-wind) in order to minimize wind acceleration effects, make plots of altitude vs time, and take slopes in order to determine dH/dt for that altitude (Fig. 13.4). Once we have this information we are ready to start one of the reduction methods.

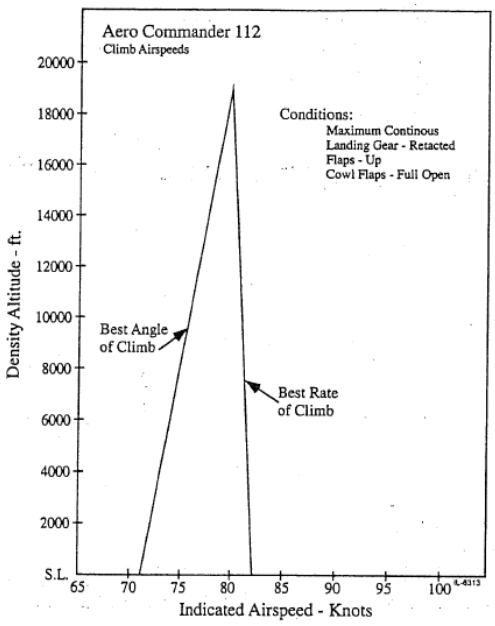

Fig. 13.3 Best rate-of-climb and best angle-of-climb airspeed vs altitude. Reprinted with permission from Commander Aircraft.

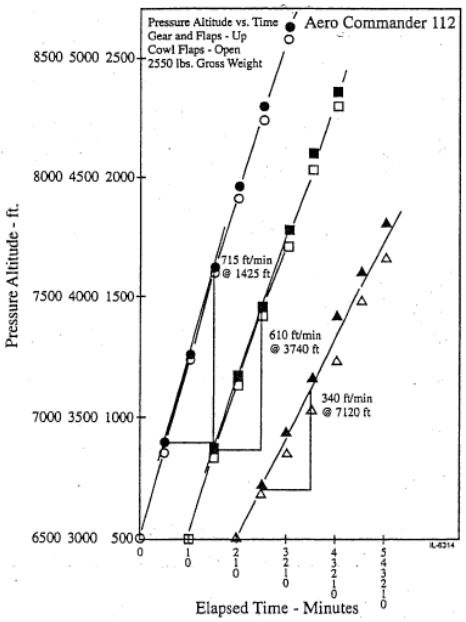

Fig. 13.4 Check climbs at V_y and three altitudes. Reprinted with permission from Commander Aircraft.

2.5.2.2 Single Heading Climbs with INS

Since the advent of the Inertial Navigation System (INS) some testing has been conducted using sawtooth climbs on only one heading.[5] Resultant data indicate that (if certain onboard test stability criteria are observed along with the use of the INS for kinetic energy corrections) the single heading method adequately defines climb performance without compromising accuracy.

2.5.3 Reduction Methods for Steady Climb

There are many accepted methods for steady climb data reduction; some are:

1) PIW vs CIW method
2) density altitude method[4]
3) equivalent attitude method[4]
4) dimensionless method[6]

The PIW vs CIW method and equivalent altitude method are simple and straightforward. The density altitude method is more complicated. All of these three methods are essentially methods for propeller-driven airplanes. PIW vs CIW and equivalent altitude are used with both constant speed-propellers and fixed-pitch propellers, while density altitude is used with constant speed-propellers.

The reduction scheme for PIW vs CIW is shown in Table 13.1. Once we have values for PIW and CIW for several altitudes we plot them as shown in Fig. 13.5. We may then obtain the maximum rate of climb at sea level and are ready to expand the data to nonstandard conditions.

The reduction scheme for the density altitude method is shown in Table 13.2. Since this method uses density altitude as a parameter, its final results plot in density altitude vs rate of climb.

The data reduction approach for the equivalent altitude method is shown in Table 13.3. This method also plots out directly into equivalent altitude vs rate of climb.

The dimensionless method of climb plotting may be used for both propeller-driven and jet aircraft, however it is used more frequently with jet aircraft.

Through dimensional analysis it can be shown that:[6]

$$\frac{FHP_R}{\delta\sqrt{\theta}} = f(M, W/\delta) \tag{13.1}$$

and

$$\frac{FHP_A}{\delta\sqrt{\theta}} = \left(\frac{F_{na}}{\delta}\right)KM = f(N/\sqrt{\theta}, M) \tag{13.2}$$

where

FHP_R = thrust horsepower required
FHP_A = thrust horsepower available
F_{na} = net thrust available
K = constant to correct M to $V/\sqrt{T_a}$

From these equations it may also be shown that:

Propeller driven

$$\frac{dH/dt}{\sqrt{\theta}} = f\left(\frac{FHP_a}{\delta\sqrt{\theta}}, M, W/\delta\right) \tag{13.3}$$

or

Turbojet

$$\frac{dH/dt}{\sqrt{\theta}} = f\left(\frac{F_{na}}{\delta}, M, W/\delta\right) \tag{13.4}$$

Figs. 13.6, 13.7, and 13.8 (Ref. 6) show typical dimensionless climb data plots.

Table 13.4 gives a method of climb data reduction for jet aircraft.

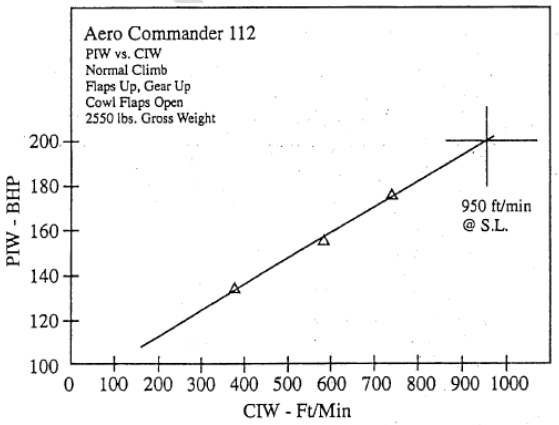

Fig. 13.5 Plot of PIW vs CIW showing sea level rate of climb. Reprinted with permission from Commander Aircraft.

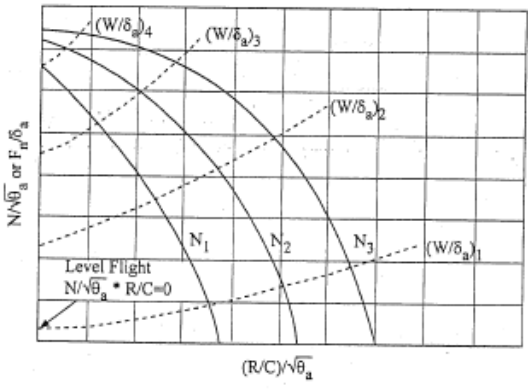

Typical Dimensionless Climb Data at Constant Mach Number and Various W/δ_a Parameters

Fig. 13.6 Typical dimensionless climb data at constant Mach number.[6]

Table 13.1 PIW-CIW data reduction and expansion

Step number	Quantity	Reference	Units	Climb #1	Climb #2	Climb #3
1	V_O	flight data	kn			
2	V_I	instrument calibration	kn			
3	V_C	position calibration	kn			
4	H_{P_O}	flight data	ft			
5	H_{PI}	instrument calibration	ft			
6	$T_O(OAT)$	flight data	°C			
7	T_I	instrument calibration	°C			
8	T_a	273.16 + #7	K			
9	CAT_O	flight data	°C			
10	CAT_I	instrument calibration	°C			
11	rpm_O	flight data	rpm			
12	rpm_I	instrument calibration	rpm			
13	$M.P._O$	flight data	in.Hg			
14	$M.P._I$	instrument calibration	in.Hg			
15	dry/wet temperature	flight data	°– / °–			
16	$\Delta M.P.$	psychrometer chart	in.Hg			
17	Effective $M.P.$	#14 – #16	in.Hg			
18	T_S at H_{PI}	altitude table	K			
19	T_{CAT}	273.16 + #10	K			
20	T_S/T_{CAT}	#18/#19	n/d			
21	$(T_S/T_{CAT})^{1/2}$	$(\#20)^{1/2}$	n/d			
22	$BHP_{ALT.}$	engine chart	hp			
23	BHP_{TC}	#22 × #21	hp			
24	δ at H_{PI}	altitude table	n/d			
25	θ	#8/288.16	n/d			
26	σ	#24/#25	n/d			
27	$(\sigma)^{1/2}$	$(\#26)^{1/2}$	n/d			
28	W_T	flight data	lb			
29	W_S	arbitrary	lb			
30	W_T/W_S	#28/#29	n/d			
31	$(W_T/W_S)^{1/2}$	$(\#30)^{1/2}$	n/d			
32	$(W_T/W_S)^{3/2}$	$(\#30)^{3/2}$	n/d			
33	PIW	(#23 × #27)/#32	hp			
34	$(dH/dt)_O$	flight data	ft/min			
35	$(dH/dt)_{TC}$	(#34 × #8)/#18	ft/min			
36	CIW	(#35 × #27)/#31	ft/min			
37	plot PIW vs CIW	#33 vs #36	——	——	——	——

Table 13.2 Climb data reduction by the density altitude method

Step number	Quantity	Reference	Units	Climb #1	Climb #2	Climb #3
1	V_O	flight data	kn			
2	V_I	Instrument calibration	kn			
3	V_C	position correction	kn			
4	H_{PO}	flight data	ft			
5	H_{PI}	instrument calibration	ft			
6	$T_O(OAT)$	flight data	°C			
7	T_I	instrument calibration	°C			
8	T_a	273.16 + #7	K			
9	T_S at H_{PI}	altitude table	K			
10	δ at H_{PI}	altitude table	n/d			
11	θ	#8/288.16	n/d			
12	σ	#10/#11	n/d			
13	$(\sigma)^{1/2}$	$(\#12)^{1/2}$	n/d			
14	V_T	#3/#13	kn			
15	H_D	$145539(1-(\#13)^{0.4659})$	ft			
16	$(dH/dt)_O$	flight data	ft/min			
17	T_a/T_S	#8/#9	n/d			
18	$(dH/dt)_T$	#16 × #17	ft/min			
19	W_T	flight data	lb			
20	W_S	arbitrary	lb			
21	R/C_{WC}	#18(1 – #19/#20)	ft/min			
22	b	airplane geometry	ft			
23	e	Oswald's efficiency factor	n/d	0.8	0.8	0.8
24	$q\pi eb^2$	$(\#3)^2\pi(\#23)(\#22)^2/295$	lb			
25	ΔD_i	$((\#20)^2 - (\#19)^2)/\#24$	lb			
26	R/C_D	101.27(#25)(#14)/#20	ft/min			
27	rpm_O	flight data	rpm			
28	rpm_I	instrument calibration	rpm			
29	$M.P._O$	flight data	in.Hg			
30	$M.P._I$	instrument calibration	in.Hg			
31	$C.A.T._O$	flight data	°C			
32	$C.A.T._I$	instrument calibration	°C			
33	$C.A.T._a$	#32 + 273.16	K			
34	$(T_I/C.A.T._a)^{1/2}$	$(\#9/\#33)^{1/2}$	n/d			
35	BHP at H_{PI}	engine power chart	BHP			
36	BHP_T	#35 × #34	BHP			
37	T_S at H_D	altitude table	K			
38	inlet heat rise	#33 – #8	K			
39	BHP at H_D	engine power chart	BHP			
40	$(T_S/C.A.T._a)_D^{1/2}$	$(\#37/(\#37 + \#38))^{1/2}$	n/d			
41	BHP_{TD}	#39 × #40	BHP			
42	η_P	propeller charts[a]	%			

Table 13.2 Climb data reduction by the density altitude method (continued)

Step number	Quantity	Reference	Units	Climb #1	Climb #2	Climb #3
43	ΔTHP	#42 × (#41 – #36)	hp			
44	R/C_{THP}	#43 × 33,000/#20	ft/min			
45	$(dH/dt)_S$	#18 – #21 – #26 + #44	ft/min			
46	H_D vs $(dH/dt)_S$	plot #15 vs #45	——	——	——	——

[a]If a propeller chart is not available this item may be estimated. At climb airspeeds values may be between 0.65 and 0.75.

Table 13.3 Climb data reduction by the equivalent altitude climb method

Step number	Quantity	Reference	Units	Climb #1	Climb #2	Climb #3
1	V_O	flight data	kn			
2	V_I	instrument calibration	kn			
3	V_C	position correction	kn			
4	H_{PO}	flight data	ft			
5	H_{PI}	instrument calibration	ft			
6	$T_O(OAT)$	flight data	°C			
7	T_I	instrument calibration	°C			
8	T_a	#7 + 273.16	K			
9	δ at H_{PI}	altitude table	n/d			
10	θ	#8/288.16	n/d			
11	σ	#9/#10	n/d			
12	$(\sigma)^{1/2}$	$(\#11)^{1/2}$	n/d			
13	H_D	$145539(1 - (\#12)^{0.4699})$	ft			
14	H_e	#5 – 0.36(#5 – #13)	ft			
15	T_S at H_{PI}	altitude table	K			
16	T_a/T_S	#8/#15	n/d			
17	$(dh/dt)_O$	flight data	ft/min			
18	R/C_{TC}	#16 × #17	ft/min			
19	W_T	flight data	lb			
20	W_S	arbitrary	lb			
21	W_T/W_S	#19/#20	n/d			
22	R/C_{WC}	#18 × #21	ft/min			
23	$(W_T/W_S)^2$	$(\#21)^2$	n/d			
24	$1 - (W_T/W_S)^2$	1 – #23	n/d			
25	b	aircraft geometry	ft			
26	e^a	Oswald's efficiency factor	n/d	0.8	0.8	
27	K	$(9504.8 \times \#20)/\#26 \times (\#25)^2$				
28	$K/V_C(\sigma)^{1/2}$	#27/#3×#12				
29	ΔD_i	#24 × #28	ft/min			
30	$(dH/dt)_S$	#22 – #29	ft/min			
31	H_e vs $(dH/dt)_S$	plot #14 vs #30	——	——	——	

[a]If actual Oswald's efficiency factor use in place of 0.8, otherwise use 0.8.

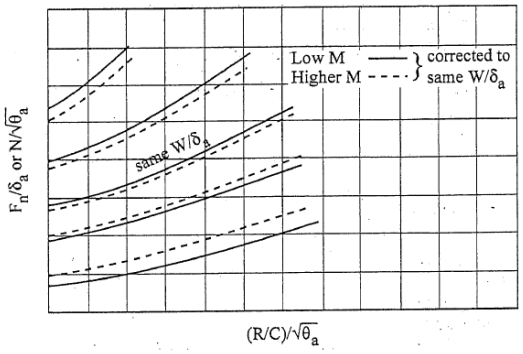

Fig. 13.7 Typical dimensionless climb data plot for two Mach numbers.[6]

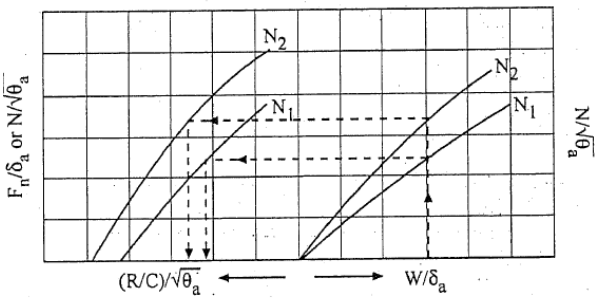

Fig. 13.8 Dimensionless climb data corrected to constant W/δ_a (Ref. 6).

Table 13.4 Jet aircraft climb data reduction[3]

Step number	Quantity	Reference	Units	Climb #1	Climb #2
1	H_{PO}	flight data	ft		
1	H_{PI}	instrument correction	ft		
3	H_{PC}	position correction	ft		
4	V_O	flight data	kn		
5	V_I	instrument correction	kn		
6	V_C	position correction	kn		
7	M	chart 8.5[3] & #6 and #3	Mach		
8	V_{TS}	chart 8.5[3] & #6 and #3	kn		
9	T_O	flight data	°C		
10	T_I	instrument calibration	°C		
11	T_{ai}	chart 8.2[3] & #10 and #7	K		
12	$\theta^{1/2}$	$(\#11/288.16)^{1/2}$	n/d		
13	$\theta_S^{1/2}$ at H_{PC}	altitude tables	n/d		
14	$(T_{ai}/T_{aS})^{1/2}$	#12/#13	n/d		
15	W_T	flight data	lb		
16	W_S	arbitrary	lb		
17	ΔW	#16 − #15	lb		
18	$\Delta W/Engine$	#17/number of engines	lb		
19	$W_T/Engine$	#15/number of engines	lb		
20	dH/dt	flight data	ft/min		
21	$(dH/dt)_{TC}$	#20 × #14	ft/min		
22	wind gradient	chart 5.41[3] when required	n/d		
23	$(dH/dt)_W$	#21 × #22 when required	ft/min		
24	acceleration factor	chart 5.51[3] for constant V_C climb	n/d		
24-1	acceleration factor[a]	chart 5.51 & 5.52 for non-constant V_C climb	n/d		
25	N_O	engine rpm - flight data	rpm		
26	N_I	instrument correction	rpm		
27	N_T	average of all engines	rpm		
28	$N_T/\theta^{1/2}$	#27/#12	rpm		
29	$N_T/\theta_S^{1/2}$	#27/#13	rpm		
30	$\Delta F_N/\delta_a$[a]	chart like 5.21[3] & #28, #29 & #7			
31	$(\Delta R/C_1)/(\Delta F_N/\delta_a)$	chart 5.22,[3] #3, #7 & #19			
32	$(\Delta R/C_1)_a$	(#31 × #30)/#24	ft/min		
33	R/C_1	#21 or #23 + #32	ft/min		
34	$\Delta R/C_2$	(−#17 × #33)/#15	ft/min		
35	$(\Delta R/C_3)\Delta W$	chart 5.31,[3] #3, #7 and wing span			
36	$(\Delta R/C_3)_a$	(#35 × #17)/#24	ft/min		
37	R/C_S	#33 + #34 + #36	ft/min		
38	H_{PC} vs R/C_S	plot #3 vs #37			

2.6 Turning (Maneuvering) Performance Methods and Data Reduction

The measurement of turning performance is of primary importance in the evaluation of combat aircraft, since the turn radius R and turn rate w are very important in air combat. For other aircraft turning performance is not so important and in many cases is ignored. This is true of most civilian aircraft and there are no current FAA regulations for turning performance.

For military fighter and attack type aircraft, a certain level of turning performance is specified in the contract. It is then up to the flight test organization to determine if this level of performance has been met.

2.6.1 Forces on an Aircraft During Level Turn

Fig. 15.1 shows the forces acting on an aircraft during a level turn. The centrifugal force F_c of the turn can be expressed by the equation:

$$F_C = ma = \frac{W}{g}\frac{V_T^2}{R} \tag{15.1}$$

where
m = mass
a = acceleration
W = weight
V_T = true airspeed
g = acceleration due to gravity
R = radius of turn

The load factor n can be derived as follows:

$$(nW)^2 = (F_C)^2 + W^2 = \left(\frac{WV_T^2}{gR}\right)^2 + W^2 \tag{15.2}$$

$$n^2 = \frac{V_T^4}{g^2R^2} + 1 \tag{15.3}$$

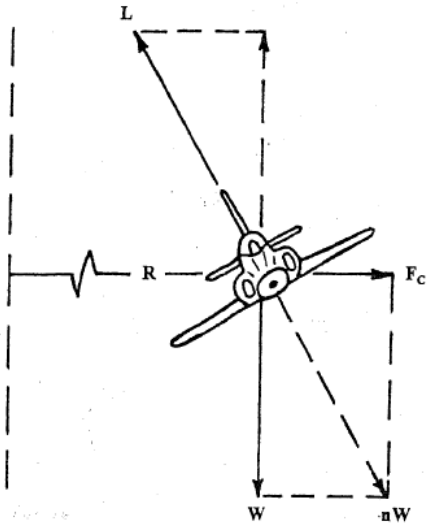

Fig. 15.1 Forces acting on an aircraft in a level turn.

The radius of turn R can be obtained by solving the above equation for R.

$$R = \frac{V_T^2}{g\sqrt{n^2 - 1}} \tag{15.4}$$

The rate of turn is obtained from:

$$\omega = \frac{V_T}{R} = \frac{g\sqrt{n^2 - 1}}{V_T} \tag{15.5}$$

where
ω is in rad/s

From flight tests we are able to obtain accurate values of V_T and ω. We can then enter Eq. (15.5) and solve for the load factor n. With this information we can enter Eq. (15.4) and solve for the turn radius R. We may then obtain plots of load factor vs airspeed and radius of turn vs airspeed for various altitudes as is shown in Figs. 15.2 and 15.3. We may then use the values obtained in level turns at constant airspeed to compare with contract specifications or other aircraft.

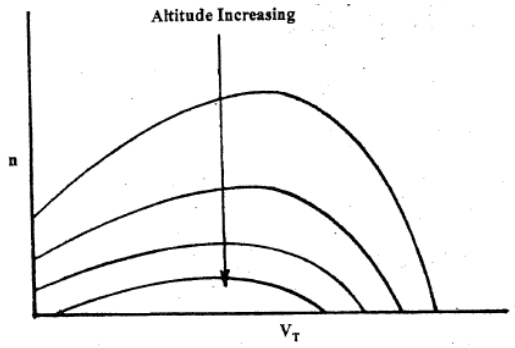

Fig. 15.2 Turning load factor vs true airspeed.

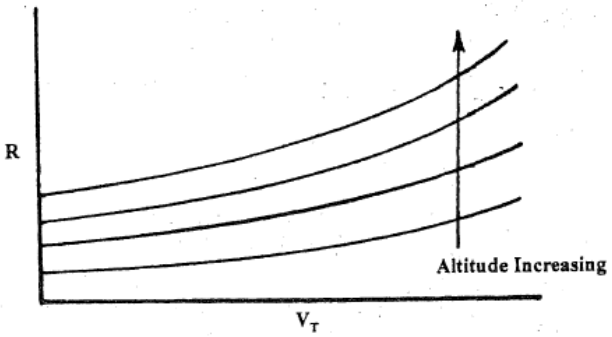

Fig. 15.3 Turn radius vs true airspeed.

2.6.2 Turning Performane Limitations

There are four primary limitations on the turning performance of an airplane. They are:

1) thrust available
2) drag characteristics
3) C_{Lmax}
4) structural strength

2.6.2.1 Thrust and Drag Limitations

In the combat situation thrust and drag are the limiting factors on continuous turns without altitude loss. Since the drag must increase in the turn due to the increased load factor, the excess thrust available will decrease for any given flight speed. Eq. (15.4) shows that the greater the load factor the smaller the level turn radius for a given true airspeed. However, the greater the load factor the greater the drag and the smaller the excess thrust, so any of the factors that affect thrust or drag affect turning performance. Corrections must therefore be applied to turning performance data for:

1) temperature effects on thrust
2) pressure altitude effects on thrust
3) weight effects on induced drag, which are multiplied by increased load factor
4) effects on the test load factor resulting from nonstandard temperature, altitude, and weight

The effects of these variables are shown in Fig. 15.4.

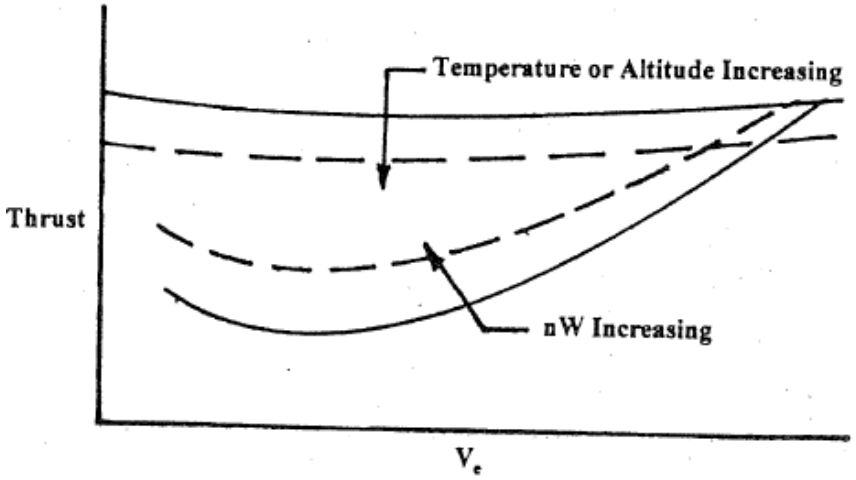

Fig. 15.4 Factors affecting turning performance.

2.6.2.2 C_{Lmax} Limitations

The C_{Lmax} limitation on turning performance occurs during that portion of the flight envelope where the load factor that the aircraft can pull is limited by aerodynamic stall or other angle of attack limitation. This limitation covers the low-speed portion of the flight envelope as is illustrated by the airspeed, V, vs load factor, n, diagram shown in Fig. 15.5.

All aircraft are capable of being flown to this limitation, and flight test to determine it are called lift boundary investigations.

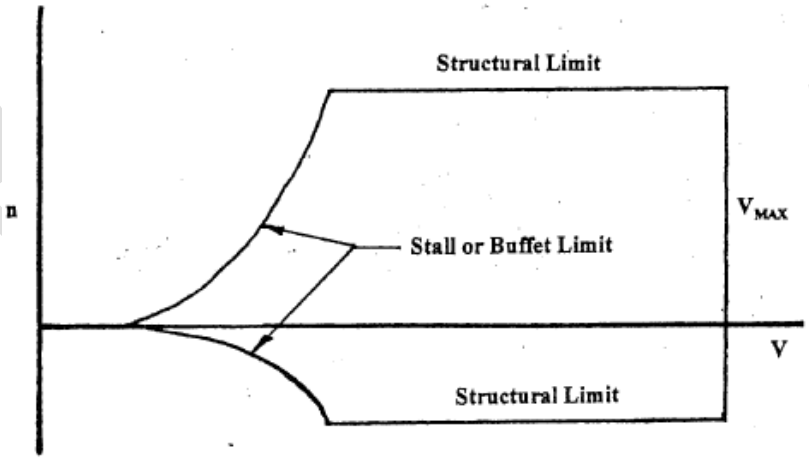

Fig. 15.5 Airspeed vs load factor (V-n) diagram.

2.6.2.3 Structure Limitaions

Structural limitations on turning performance have not been a significant factor on older combat aircraft, since most were not capable of achieving their limit load factor in a level turn. They are becoming more of a factor on today's aircraft that have high power-to-weight ratios and are capable of sustaining the

limit load factor in level flight through a larger portion of the flight envelope.

As we can see from Eq. (15.4), once we have reached limit load factor the turn radius will increase as true airspeed increases. The reverse is true of turn rate as can be seen from Eq. (15.5).

2.6.3 Flight Test Method

2.6.3.1 Preflight Procedure

A pilot's data card should be prepared for the recording of the following data in each stabilized turn:

observed airspeed (V_o)
observed pressure altitude (H_{P_o})
normal acceleration (n_Z)
fuel used or remaining (W_F)
outside air temperature (T_o)

In addition, the card should contain a table of how n_Z varies with bank angle, ϕ. It is also helpful if a blank plot of n_Z vs V_o is available so the pilot can make a rough "how goes it" plot during the flight.

2.6.3.2 Data Collection

Once data have been collected at several different altitudes they may be reduced using the following procedure:

1) Apply instrument and position corrections. Be sure to apply any tare correction to n_Z data.
2) Determine the aircraft test gross weight, W_T.
3) Correct n_Z to standard weight.

$$n_{z_S} = n_{z_T}\left(\frac{W_T}{W_S}\right) \tag{15.6}$$

4) Construct a plot of n_{ZS} vs M or V_T.
5) Calculate turn radius, R, from Eq. (15.4).
6) Calculate turn rate, ω, from Eq. (15.5).
7) Plot n_{Z_S} vs M or V_T.
8) Plot R vs M or V_T.
9) Plot ω vs M or V_T.

2.6.3.3 Normalization

In many cases it may not be possible to obtain complete data for turning performance due to the amount of data required. However, Perkins and Dommasch[3] show that:

$$\frac{n_Z W}{\delta} = f(M, F_N/\delta) \tag{15.7}$$

From this functional relation we can see that for constant values of W, M, and F_N/δ the normal load factor n_Z is a direct function of the atmospheric pressure ratio δ. Through this relationship the turning performance at one altitude may

be related to the turning performance at any other altitude, or:

$$\frac{n_{Z1}}{n_{Z2}} = \frac{\delta_1}{\delta_2} \tag{15.8}$$

A plot demonstrating this ratio is shown in Fig. 15.6.

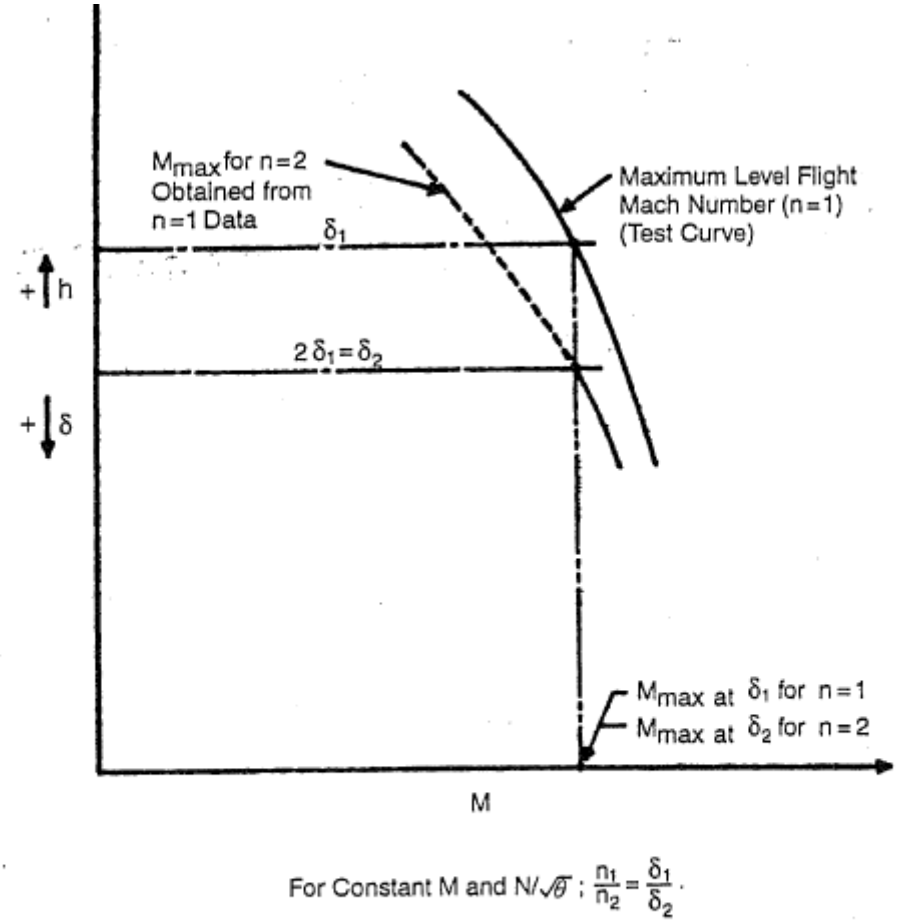

Fig. 15.6 Plot of altitude vs Mach showing load factor and pressure ratio relation.[3] [The original version of this material was first published by the Advisory Group for Aerospace Research and Development, North Atlantic Treaty Organization (AGARD/NATO) in *AGARD Flight Test Manual, Volume I—Performance.*]

2.7 Methods of Drag determination in Flight

An accurate determination of drag is one of the most difficult tasks undertaken in flight testing. It is, however, a very important item since if the drag polar of an aircraft is accurately determined and the thrust, or thrust horsepower, available is known then all of the performance characteristics of the subject airplane may be calculated.

There are a number of methods for determining drag through flight testing. The objective of this discussion is to examine several of these methods. We will discuss the theory of the methods along with the strengths and weaknesses of each.

The four methods we will investigate are:

1) speed power method
2) prop-feathered sinks method
3) incremental drag method
4) incremental power method

2.7.1 Speed Power Method (Drag Polar)

This method is based on the fact that for level, unaccelerated flight thrust is equal to drag. Therefore, if we can determine the thrust, or thrust horsepower, at a given level flight speed, we may also determine the drag at that given speed. Since we have already discussed the theory behind the speed power or PIW-VIW method, we will not repeat it here.

The equation on which the speed power polar is based is:

$$\frac{BHP_{REQ}\sqrt{\sigma}}{(W_T/W_W)^{3/2}} = f\left(\frac{V_T\sqrt{\sigma}}{\sqrt{W_T/W_S}}\right) \tag{16.1}$$

The left side of this equation is called PIW and the right side VIW. A typical plot of this curve is shown in Fig. 16.1. For a given configuration and propeller the PIW-VIW plot will define speed power performance at any altitude and weight. From the PIW-VIW plot we may obtain the drag polar for the airplane by using the following equations for drag and lift coefficients:

$$C_D = \frac{2(550)(PIW)\eta_P}{\rho_0(VIW)^3 S} \tag{16.2}$$

$$C_L = \frac{2W_S}{\rho_0(VIW)^2 S} \tag{16.3}$$

where

$\rho_0 = .00237$ slugs/ft^3
C_D = drag coefficient
η_P = propeller efficiency
S = wing area
C_L = lift coefficient

The propeller efficiency η_P may be assumed to be a constant value such as 0.83 or determined for each point from propeller efficiency charts. The latter method being the most accurate.

Plots of C_D vs C_L and C_D vs C_L^2 developed by the above methodology from the data in Fig. 16.1 are shown in Figs. 16.2 and 16.3.

The strength of this method is that it is relatively simple to perform, and the data is easy to reduce. It also does not require sophisticated instrumentation to obtain reasonable data.

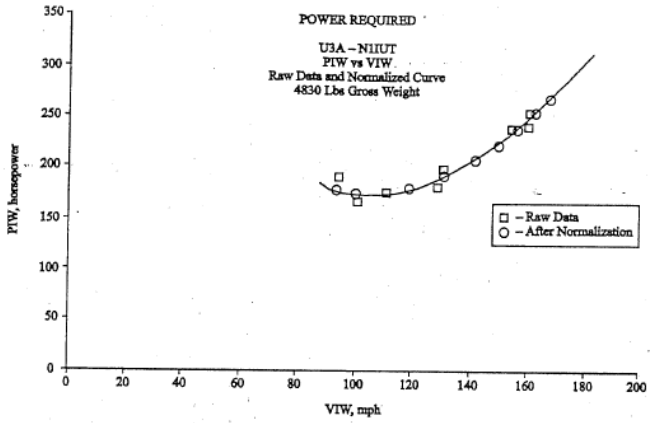

Fig. 16.1 PIW vs VIW plot for Cessna U3A.

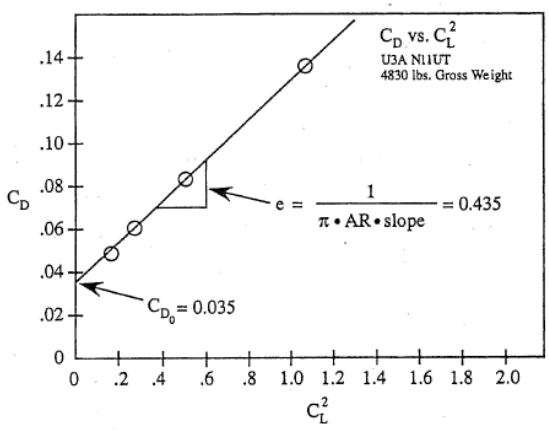

Fig. 16.2 Plot of C_D vs C_L^2 for Cessna U3A.

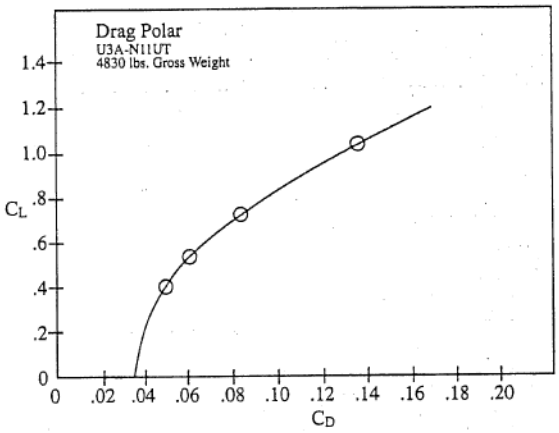

Fig. 16.3 Plot of C_L vs C_D for Cessna U3A.

Its problems fall in the area of determining the installed power and in assuming that propeller efficiency remains constant, which it does not. Installed power is difficult to determine without the use of torque meters or other devices and most of these have some limits on their accuracy. Propeller efficiency is also difficult to accurately determine and recent full-scale wind tunnel tests of the Advanced Technology Light Twin (ATLIT) have shown that the old methods, such as Gray Charts, have yet to be much improved on.

For a jet aircraft, speed power data is obtained using the constant W/δ method. As was discussed in that section, drag may be extracted directly from the flight test data.

The strengths of the method for jet aircraft are the same as for propeller-driven aircraft. Its problem is an accurate determination of installed thrust.

2.7.2 Prop-Feathered Sink or Glde Polars

2.7.2.1 Federal Aviation Administration Requirements

Prior to 1996 neither CAR 3 nor FAR Part 23 contained requirements for glide performance. However, in 1996 the FAA added FAR 23.71 entitled "Glide: Single-Engine Airplanes." This regulation required that the maximum horizontal distance traveled in still air per 1000 ft of altitude lost be determined in nautical miles. The speed to achieve this distance is to also be determined with the engine inoperative and the landing gear and flaps in the most favorable position. The propeller is to be in the minimum drag position.

2.7.2.2 Theory

If we examine the forces acting on an airplane in a steady-state glide (Fig. 16.4) we can see that the only forces remaining to vectorially balance the weight are the lift and the drag. In examining Fig. 16.4 we can see that, in this case:

$$L = W_T \cos\gamma \tag{16.4}$$

$$D = -W_T \sin\gamma \tag{16.5}$$

Then from the flight test we need to know the glide angle γ, and the test weight W_T.

In order to determine the glide angle γ we must determine the rate-of-descent dH_p/dt and the true airspeed V_T. Glides are usually made through the same altitude increment at several different airspeeds in order that a plot of

rate of descent vs airspeed can be constructed (Fig. 16.5). It is from this plot that the drag polars may be generated by use of Eqs. (16.4) and (16.5) and the coefficients obtained by the basic lift and drag equations.

In order to obtain the rate of descent vs airspeed plot the data must first be converted to a tapeline rate of descent. This is accomplished by first correcting

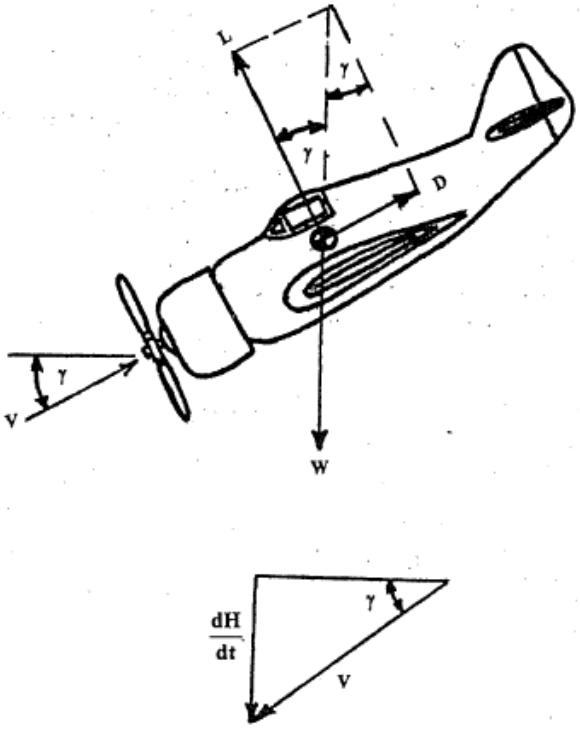

Fig. 16.4 Forces and their components during a glide.

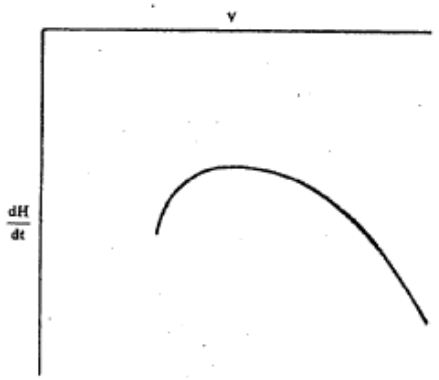

Fig. 16.5 Plot of rate of descent vs airspeed.

the rate of descent data for nonstandard temperature.

$$\left(\frac{dH}{dt}\right)_{TC} = \left(\frac{dH}{dt}\right)_{OBS}\left(\frac{T_O}{T_S}\right) \tag{16.6}$$

where
T_O = observed temperature at the test altitude
T_S = standard temperature at the test altitude

The airspeed side of the plot may be handled in the same manner as VIW.

The strengths of this method are that it is simple and straightforward, and it does not require the determination of power or propeller efficiency. It also works well for jet aircraft where the motoring characteristics of the engine may be determined.

The problems associated with the method are that for propeller-driven aircraft we cannot account for the drag due to slipstream, the drag due to the feathered propeller, or the differences in cooling drag between a cold and a hot engine. In addition, the method presents some hazard since, in most high-wing, loaded aircraft the descent is quite rapid and the time allowed for restarting the engines may be small. Therefore, it is best attempted in an area where dead stick landings can be made without difficulty.

2.7.3 Incremental Drag Method

The incremental drag method is based on the relation that:

$$FHP = DV \tag{16.7}$$

where
FHP = thrust horsepower
D = drag
V = true airspeed

and that if a known increment of drag ΔD is added, then to maintain straight and level flight at the same airspeed an increment of thrust horsepower must also be added or:

$$FHP + \Delta FHP = (D + \Delta D)V \tag{16.8}$$

If we consider that $FHP = (BHP)\eta_P$ and that change in propeller efficiency (η_P) due to the change in drag is small it can be shown that:

$$D = \Delta D\left(\frac{BHP}{\Delta BHP}\right) \tag{16.9}$$

Since the terms on the right side of the equation can be determined we may also determine drag.

Some of the problems associated with the method are: 1) obtaining the known drag increment and 2) determining power, which is essentially the same problem as in other methods.

To the author's knowledge this method is not currently being used by flight test organizations, however, Mississippi State University conducted some research into the method that, along with the derivation of Eq. (16.9), is reported in SAE Paper 770470 (Ref. 4).

2.7.4 Incremental Power Method

This method is best performed on multiengine airplanes such that exactly one half of the power can be reduced. The test is performed by establishing level flight with both engines operating at a constant airspeed. This condition may be described by our equation:

$$\eta_P BHP_2 = DV \tag{16.10}$$

where
BHP_2 = the total horsepower developed by both engines

We then feather one engine while maintaining the same airspeed and record the rate of descent. The second condition may be described by the equation:

$$BHP_1 = DV + W_T(\sin\gamma) \tag{16.11}$$

$$BHP_1 = \frac{1}{2}BHP_2 \tag{16.12}$$

Then by substitution we can show that:

$$D = -2W_T(\sin\gamma) \tag{16.13}$$

As you can see this method is similar to the prop-feathered sink method and the data reduction is the same.

The method's strength is that it is much safer than the prop-feathered sink.

It does, however, have all of the problems associated with the prop-feathered sink, while gaining one new one due to the rudder deflections required to trim

the dead engine. This may not be too significant at high airspeed since the deflection would be small, but as speed approaches minimum control speed it becomes much more significant.

2.8 Takeoff and Landing Flight Test Methods

Takeoff and landing distances are some of the most difficult and costly flight test data to obtain. They are difficult to obtain due to the large number of variables involved with some variables, such as pilot technique, being essentially uncontrollable. They are costly due to the size of the test team required, the amount of specialized test equipment required, and the amount of data reduction involved.

Also, takeoff and landing data may only be considered to be ballpark answers due to the large factor that pilot technique plays. This is especially true where less skilled pilots are involved and may be the reason why the FAA in CAR 3 and early FAR Part 23 did not have a regulatory requirement to collect takeoff and landing data for airplanes of less than 6000 lb gross weight.

For airplanes of more than 6000 lb gross weight, regulations do exist and are divided into those for light aircraft (aircraft of less than 12,500 lb gross weight) and transport aircraft (aircraft in excess of 12,500 lb gross weight). These categories are covered by FAR Part 23 for light aircraft and FAR Part 25 for transport aircraft. There are several differences between these regulations but the main difference is the obstacle height that must be cleared. For FAR Part 23 (light aircraft) it is 50 ft. For FAR Part 25 (transport aircraft) it is 35 ft for takeoff and 50 ft for landing. This seems to be reversed since the transport regulation is supposed to be a more difficult regulation with which to comply. However, if one considers the quality of airports from which these aircraft operate, one may begin to understand some of the reasoning behind it.

2.8.1 Theory

In considering either takeoffs or landings, it is customary to divide them into two segments: 1) ground distance segment; and 2) air distance segment.

2.8.2 Test Methods

There are a number of test methods used for takeoff and landing tests. These methods vary from relatively simple and inexpensive methods to very complex and expensive methods.

2.8.2.1 Slight Bar Method

One of the simplest and least expensive methods is the sighting bar method. This method consists of one or two sighting bars located at a known distance from the runway. By the use of these devices, a stopwatch, runway observers, and hand-recorded flight data, takeoff or landing data may be obtained. A typical sighting bar takeoff and landing course is shown in Fig. 18.2. Variations of this basic method include a single sighting bar that obtains both horizontal and vertical distance information. The sighting bar method is very dependent upon the observer operating the sight bar and upon the runway observers. This dependence reduces the accuracy of the method. However, the loss in accuracy is compensated for by the simplicity of the method. Since the raw data is immediately available without film reading or other preliminary reduction, it is possible to conduct more data runs and obtain a larger statistical sample.

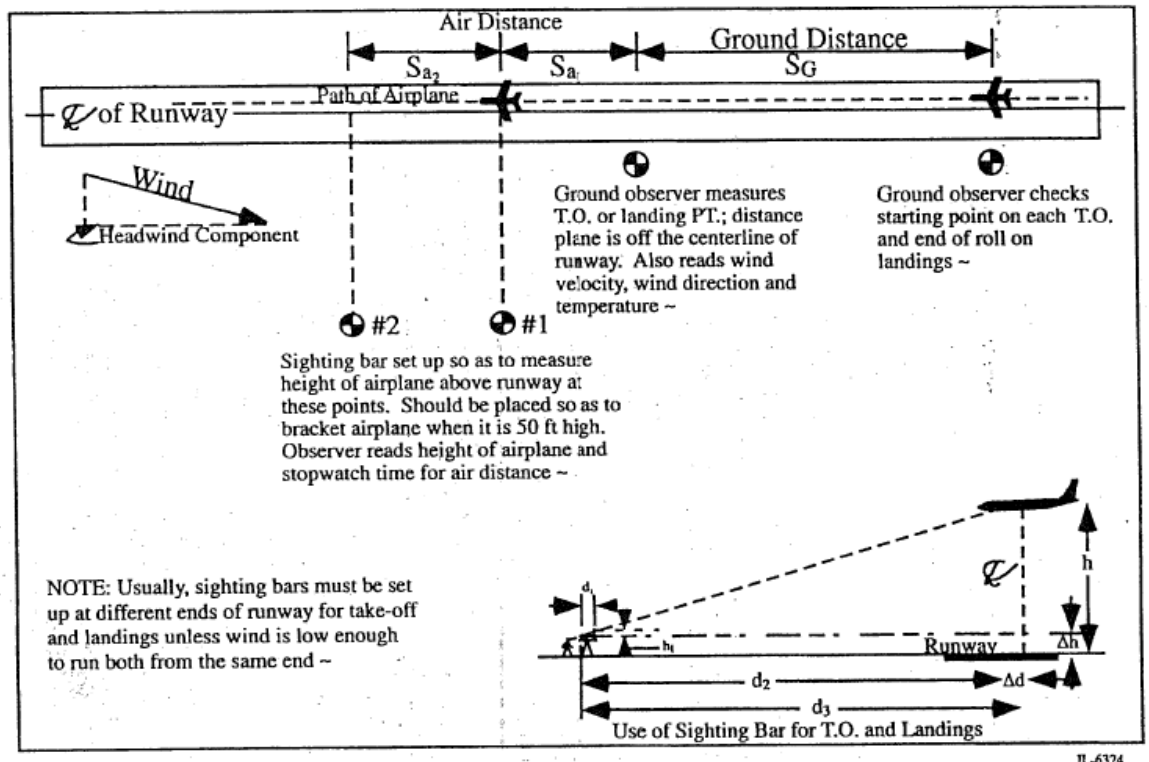

Take-Off and Landing Course (Sighting Bar)

Fig. 18.2 Sighting bar takeoff and landing course.[4]

2.8.2.2 Movie Theodolite

The movie theodolite method is similar to the strip camera method except that a movie camera is substituted for the strip camera. Fig. 18.3 shows a movie theodolite takeoff and landing course. As can be seen from this figure,

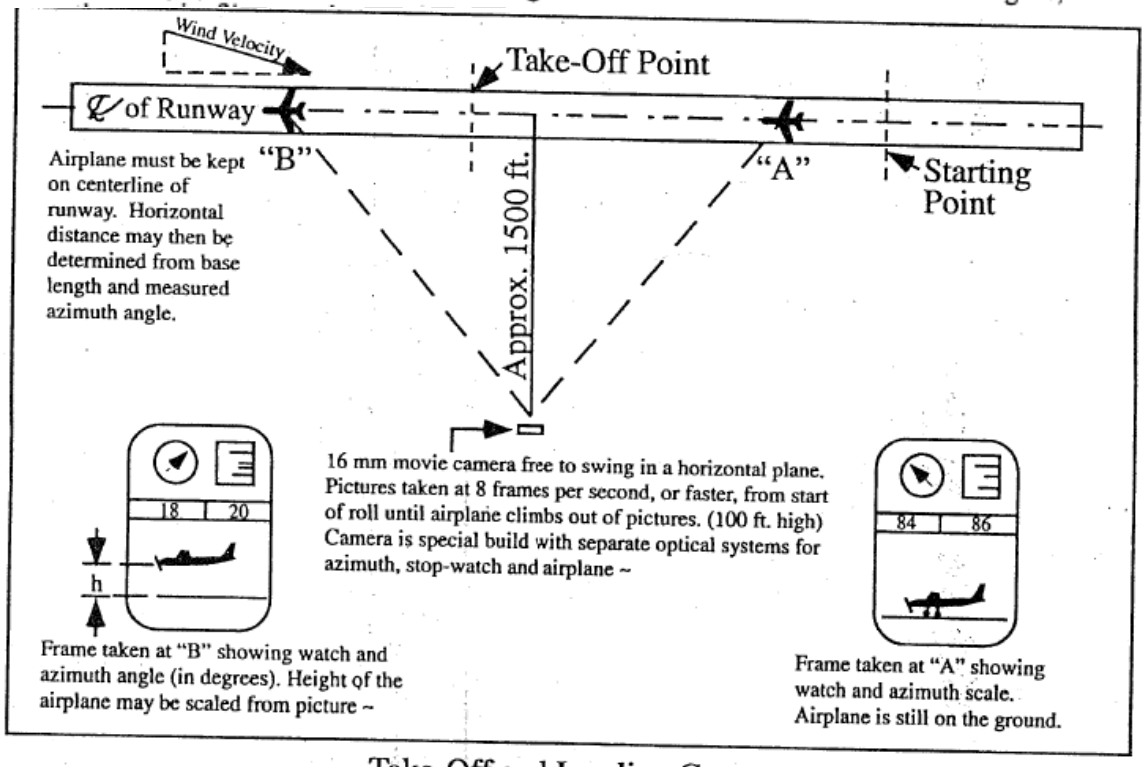

Take-Off and Landing Course

Fig. 18.3 Movie theodolite takeoff and landing course.[4]

the movie film can be used to record other data such as time and azimuth in addition to filming the airplane. This method offers accuracy equal to or slightly better than the strip camera method. Accuracy may also be improved if there is correlation between the movie theodolite and the data recording devices onboard the aircraft. This method is more sophisticated and costly than the previously discussed methods, and the data film is more difficult and time-consuming to analyze.

2.8.2.3 Strip Camera Method

The strip camera method uses a camera that takes a picture at fixed time intervals while tracking the test aircraft and records the strip picture on a photographic plate. In this manner, one takeoff or landing run is recorded on a single photographic plate as a series of strip pictures. By knowing the location of the camera site with respect to the runway, the takeoff distance and height information along with a time reference can be obtained from the photographic plate. This method is more expensive than the sighting bar method due to the cost of processing the film and obtaining the data from it. Runway observers are still required to help pin down the liftoff or touchdown point and collect wind and temperature information. This method does provide a permanent record of the takeoff or landing and is accurate.

2.8.2.4 Onboard Theodolite Method

A more recent method than those previously described is the on-board theodolite. In this method a camera is mounted on the airplane to obtain three-axis position information. Runway lights and other objects on or along the runway of known size are used with photogrammetric techniques and perspective geometry to obtain airplane position and altitude. A time readout is also displayed, usually on the edge of the film. This system also provides for easy coordination with other onboard data systems since they are all contained within the test airplane. An onboard system is expensive and requires special equipment for film analysis. It offers the advantage of not requiring a large test crew.

2.8.2.5 Del Norte Trisponder

A new system for determining takeoff and landing distances has recently been developed by Del Norte Technology, Inc., called the Trisponder 202. This unit measures horizontal distance and, when combined with a radio altimeter for height information, provides all the distance and height information necessary for determining takeoff and landing distances.

The Trisponder consists of a distance measuring unit (DMU), a master transponder, a remote transponder, and associated antennae, cables, and power sources. The master transponder and DMU can be located on the aircraft while the remote transponder is located on the ground or vice versa. If space and loading limitations allow, it is preferable to locate the DMU and master transponder onboard the aircraft since this will simplify the problem of time correlating the distance and height data.

The beauty of this system is that it does not require any surveyed test site. This allows the system to be loaded aboard the test aircraft and flown to another site should weather or traffic prevent conducting the test at the primary test site.

The drawback to the system is its initial cost and its electronic complexity.

2.8.3 Test Procedures

Since there are a large number of uncontrollable variables in takeoff and landing testing, every effort should be made to control those variables that can be controlled. First, let us look at items that apply for both takeoff and landing.

The atmospheric variables (wind, outside air temperature, and pressure altitude) should be recorded at the time of the test run for each run. The wind velocity and direction at both the 50-ft obstacle height and 6 ft above the runway should be recorded for each run. Tests should not be conducted if the wind velocity exceeds 10 kn, since wind corrections become unreliable above that wind speed.

2.8.3.1 Takeoff

Now let us turn our attention to the takeoff procedure. In order to reduce data scatter the aircraft should be stopped at the starting point, the power increased to takeoff power, allowed to stabilize, and then the brakes released. The pilot technique for ground roll, rotation, and climb should be, as nearly as possible, the same for each series of takeoffs. Experimentation to determine the optimum technique should be conducted prior to taking data and not during the actual tests.

Flight data should be collected during the entire takeoff and climb to the obstacle on a photo panel or other suitable recording device. A time reference and some method of correlating flight data with distance and height data such as event lights is also useful. If the events of brake release and liftoff are shown on both flight and height-distance data along with time, correlation between these two sets of data is greatly simplified and accuracy improved. If it is not possible to continuously collect flight data during the takeoff run then flight data should be recorded 1) just prior to brake release; 2) at liftoff; and 3) at the approximate 50-ft obstacle height.

2.8.3.2 Landing

The procedures for landing tests are somewhat like the takeoff only in a reverse direction. In the landing, test power information is not so important as in the takeoff; however, it should be monitored closely to insure that residual power does not remain after touchdown. Braking should be applied to the maximum without skidding the tires. The brakes should be given enough time to cool between runs so that they do not drag on the next takeoff or fade during the next landing. As in the takeoff, the piloting and braking technique should be as consistent as possible.

At the end of the landing run the airplane should be brought to a complete stop and held there several seconds so the end of the run may be easily identified on the film or other data trace. Event lights, or marks, are also handy in this identification.

2.8.4 Data Reduction

The final data plot for each takeoff or landing run from any of the test methods should look similar to those obtained from the Trisponder and shown in Figs. 18.4 and 18.5. Once we have this data and flight data we can start the data reduction to standard conditions.

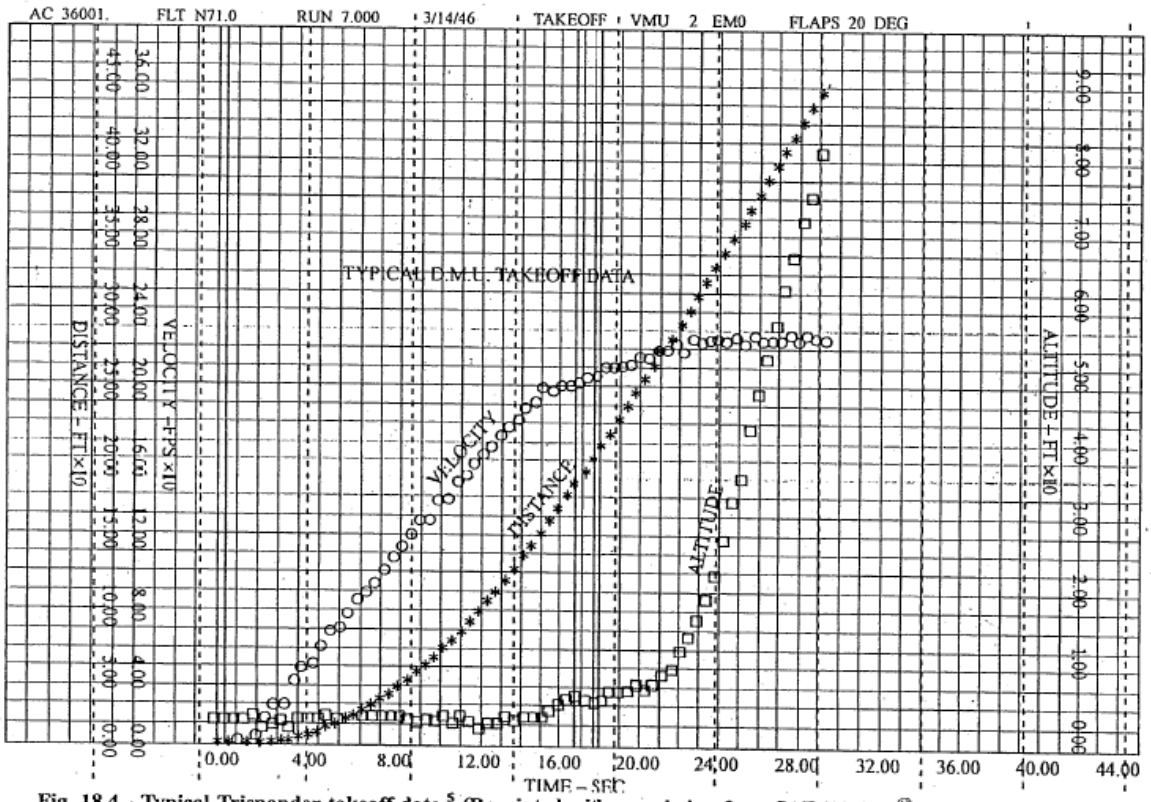

Fig. 18.4 Typical Trisponder takeoff data.[5] (Reprinted with permission from SAE 770477 ©1977 SAE International.)

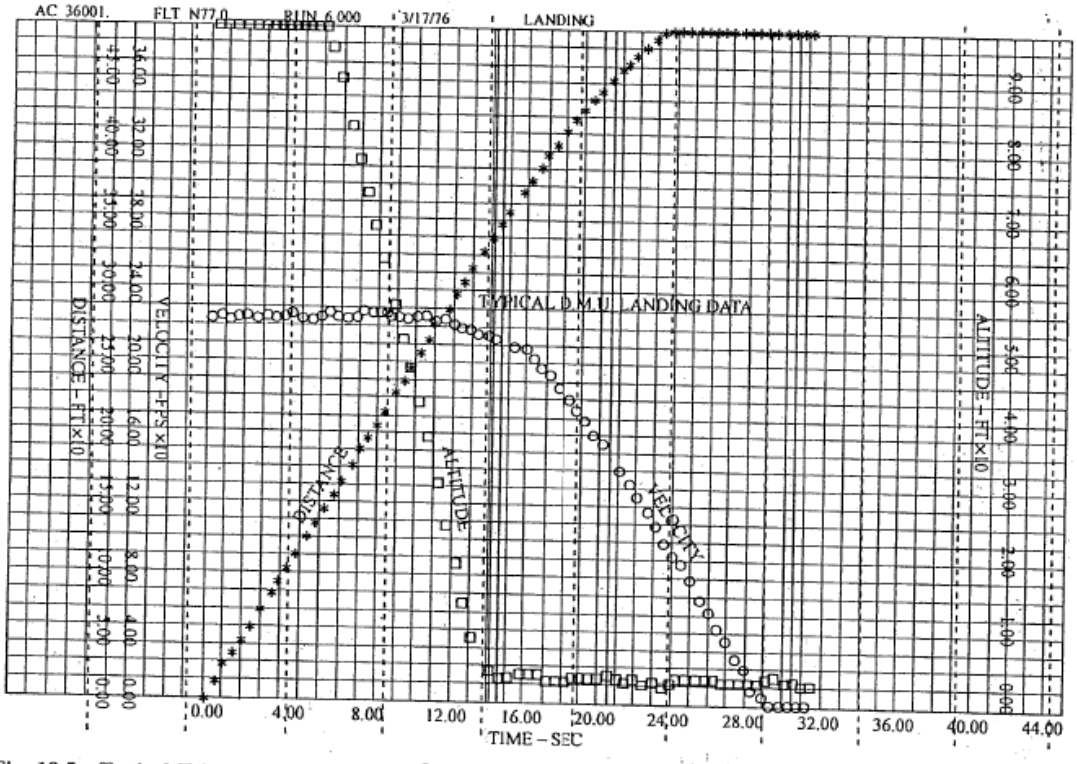

Fig. 18.5 Typical Trisponder landing data.[5] (Reprinted with permission from SAE 770477 ©1977 SAE International.)

2.8.4.1 Takeoff

The first step in reducing the takeoff data is to make the correction for wind. The wind correction must be made to both the observed ground distance S_{gO} and the observed air distance S_{aO} as shown in the following equations:

$$S_{gT} = S_{gO}\left(1 + \frac{V_W}{V_{TOw}}\right)^{1.85} \tag{18.13}$$

$$S_{aT} = S_{aO} + V_W t \tag{18.14}$$

where

S_{gT} = the test ground distance or wind corrected ground distance
S_{aT} = the test air distance or wind corrected air distance
V_W = the component of the wind velocity along the runway
V_{TOw} = the true ground speed at takeoff
t = the time from liftoff to the 50-ft obstacle

Once the wind corrected distances have been obtained it is necessary to correct the distances to sea level standard conditions. To do this by exact methods requires the knowledge of thrust, thrust minus resistance, and thrust minus drag. Since this information is not usually available for the takeoff configuration, empirical forms have been developed through experience that provide a reasonable correction. The empirical equations for correcting takeoff distances to standard conditions for jet and constant speed propeller-driven airplanes are given below. Empirical equations for other types of aircraft (fixed-pitch propeller and so on) are given in the "Flight Test Engineers Handbook."[3]

18.6.1.1 Jet aircraft.

$$S_{gS} = S_{gT}\left(\frac{W_S}{W_T}\right)^{2.3}\left(\frac{\sigma_T}{\sigma_S}\right)\left(\frac{F_T}{F_S}\right)^{1.3} \tag{18.15}$$

$$S_{aS} = S_{aT}\left(\frac{W_S}{W_T}\right)^{2.3}\left(\frac{\sigma_T}{\sigma_S}\right)^{0.7}\left(\frac{F_T}{F_S}\right)^{1.6} \tag{18.16}$$

where

S_{gS} = sea level standard ground distance
S_{aS} = sea level standard air distance
F_T = test thrust
F_S = standard thrust

18.6.1.2 Constant speed propeller-driven aircraft.

$$S_{gS} = S_{gT}\left(\frac{W_S}{W_T}\right)^{2.6}\left(\frac{\sigma_T}{\sigma_S}\right)^{1.9}\left(\frac{N_T}{N_S}\right)^{0.7}\left(\frac{BHP_T}{BHP_S}\right)^{0.5} \tag{18.17}$$

$$S_{aS} = S_{aT}\left(\frac{W_S}{W_T}\right)^{2.6}\left(\frac{\sigma_T}{\sigma_S}\right)^{1.9}\left(\frac{N_T}{N_S}\right)^{0.8}\left(\frac{BHP_T}{BHP_S}\right)^{0.6} \tag{18.18}$$

where

N_S = maximum takeoff rpm
N_T = actual rpm during the test run

Once the standard ground and air distances are obtained by one of the above methods, the standard distance over a 50-ft obstacle S_{50} is obtained by adding the air and ground distances together.

$$S_{50} = S_{gS} + S_{aS} \tag{18.19}$$

This process is done for each test run and an average taken of all the runs to determine the final distance.

After the average distances have been determined the data may be expanded to nonstandard conditions, such as those shown in Fig. 18.6, by reverse use of the above equations.

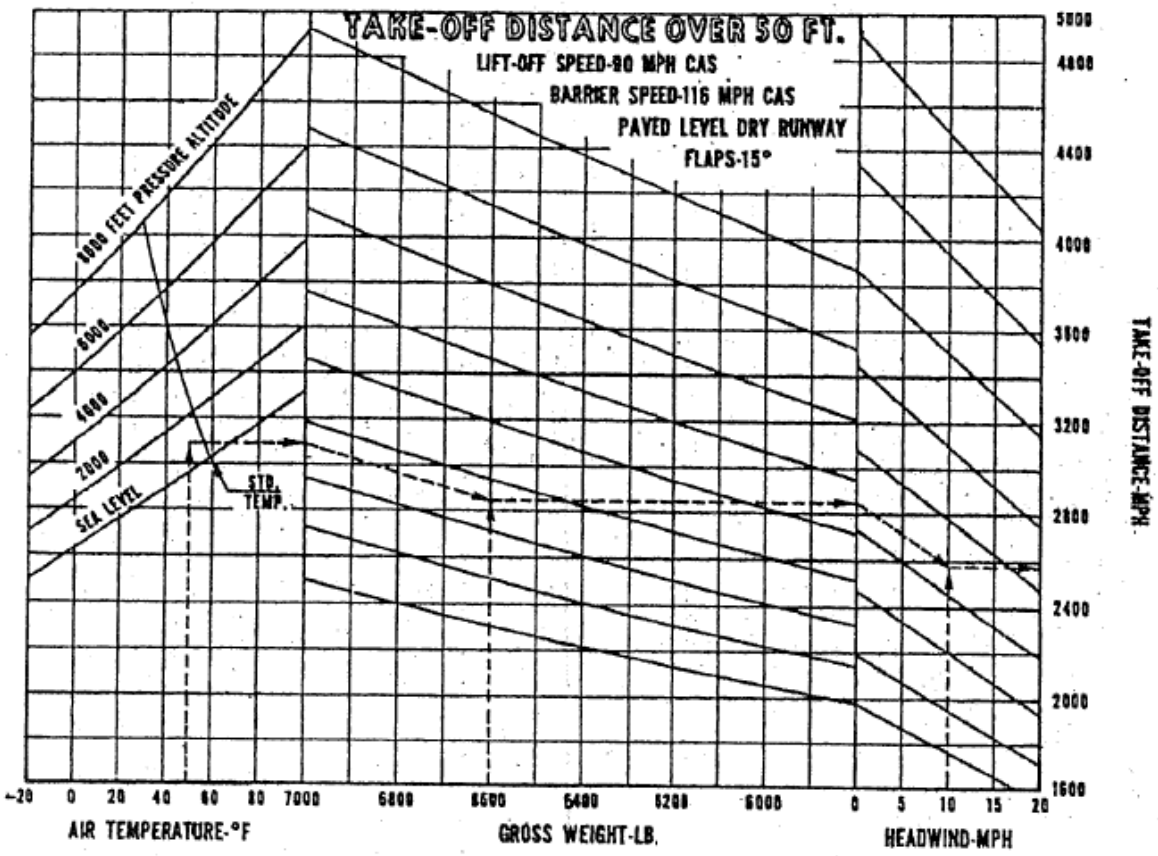

Fig. 18.6 Expanded handbook takeoff data.[6]

2.8.4.2 Landing

The correction of landing distances is much simpler than is the correction of takeoff distances. The reason for this is that the power is either at idle or held constant at some low value from the obstacle height to touchdown. This removes the power corrections from the empirical equations and greatly simplifies them.

The landing data, like the takeoff data, is first corrected for wind. The equations for wind correction of landing distances are quite similar to the takeoff wind corrections and are shown below.

$$S_{gT} = S_{gO}\left(\frac{V_{TD} + V_W}{V_{TD}}\right)^{1.85} \tag{18.20}$$

$$S_{aT} = S_{aO} + V_W t \tag{18.21}$$

where

V_{TD} = the touchdown airspeed

To correct these distances to standard conditions the following empirical equations may be used:

$$S_{gS} = S_{gT}\left(\frac{W_S}{W_T}\right)^2\left(\frac{\sigma_T}{\sigma_S}\right) \qquad (18.22)$$

It has been found that the weight correction to the landing ground distance is not accurate and that weight does not affect landing ground distance in any predictable form. For this reason landing tests are usually conducted as close to maximum gross weight as possible and the weight correction of Eq. (18.22) ignored.

$$S_{gS} = S_{gT}\left(\frac{\sigma_T}{\sigma_S}\right) \qquad (18.23)$$

$$S_{aS} = S_{aT} \qquad (18.24)$$

The total standard landing distance can then be expressed as:

$$S_{50} = S_{gT}\left(\frac{\sigma_T}{\sigma_S}\right) + (S_{aO} + V_W t) \qquad (18.25)$$

Expansion to nonstandard conditions, such as is shown in Fig. 18.7, may be accomplished by a reverse use of the correction equations.

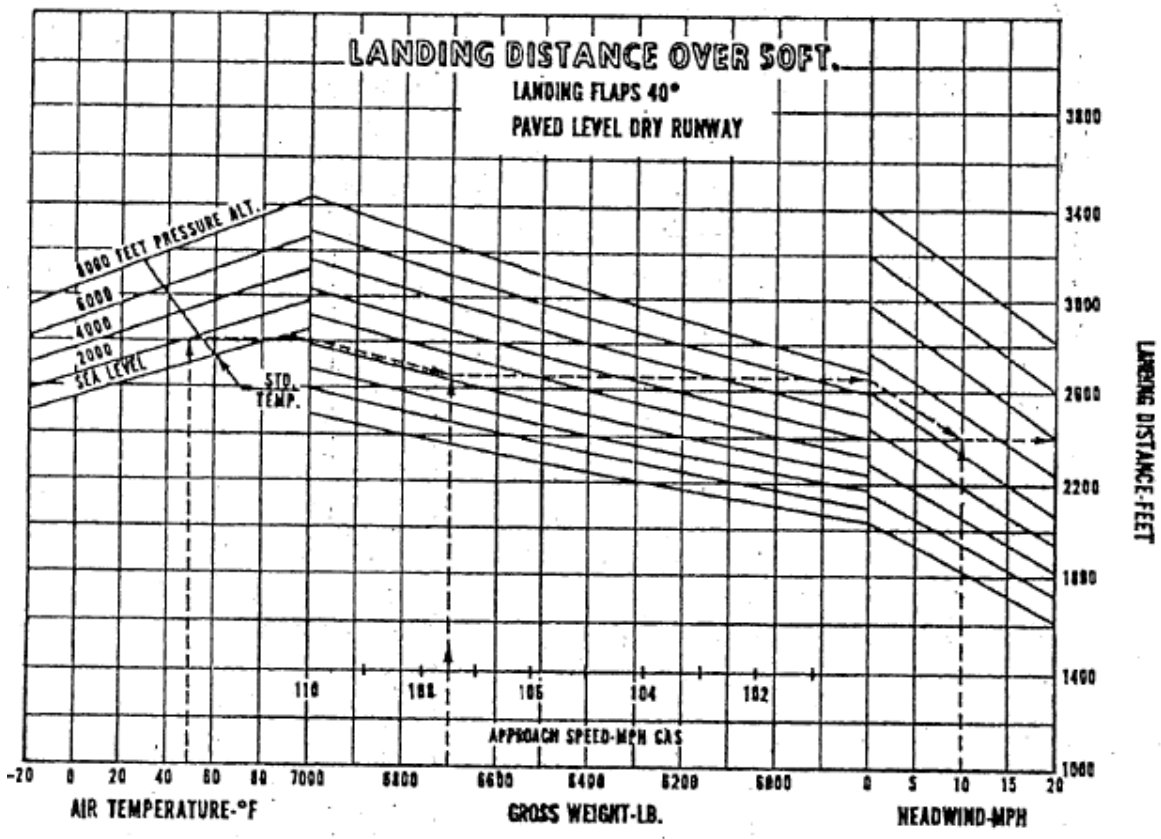

Fig. 18.7 Expanded handbook landing data.[6]

Previous exam questions:

1. (10AE831 – June/July 2018)

a. What is drag polar? Mention the methods used for determining drag through flight testing. Explain any one method. (10M)

b. Explain the flight test methods used for takeoff and landing performance evaluations.(10M)

2. (10AE831 – June/July 2017)

a. What are test methods used for takeoff and landing tests? (20M)

3. (06AE831 – June/July 2011)

a. What are test methods used for takeoff and landing tests? (20M)

3. (06AE831 – May/June 2010)

a. Explain the primary limitations on turning performance of an airplane. (20M)